

Oligonucleotide Analogues with Integrated Bases and Backbone

Part 14¹⁾

Synthesis and Association of Ethynylene-Linked Self-Complementary Tetramers

by Xiaomin Zhang, Bruno Bernet, and Andrea Vasella*

Laboratorium für Organische Chemie, ETH Zürich, Wolfgang-Pauli Strasse 10, CH-8093 Zürich
(e-mail: vasella@org.chem.ethz.ch)

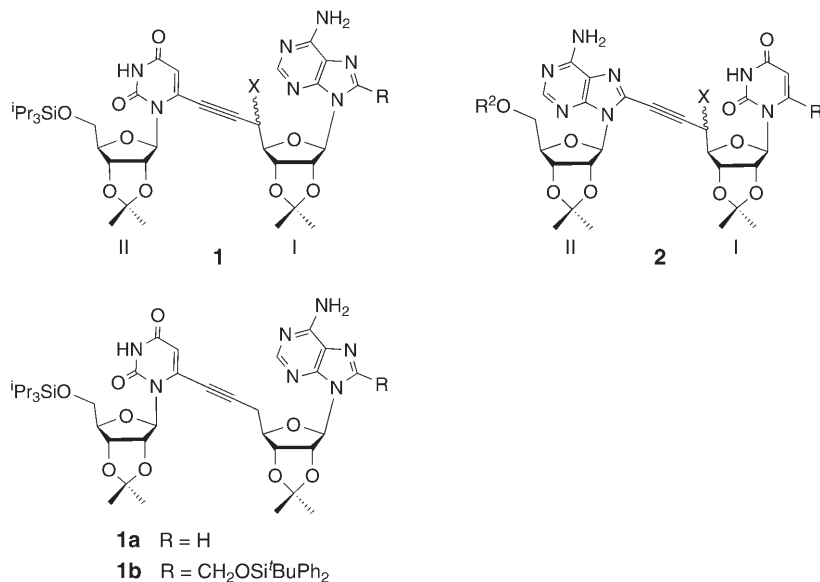
The self-complementary tetrameric propargyl triols **8**, **14**, **18**, and **21** were synthesized to investigate the duplex formation of self-complementary, ethynylene-linked UUA, AAU, UAU, and AAU analogues with integrated bases and backbone (ONIBs). The linear synthesis is based on repetitive *Sonogashira* couplings and *C*-desilylations (34–72% yield), starting from the monomeric propargyl alcohols **9** and **15** and the iodinated nucleosides **3**, **7**, **11**, and **13**. Strongly persistent intramolecular H-bonds from the propargylic OH groups to N(3) of the adenosine units prevent the *gg*-type orientation of the ethynyl groups at C(5'). As such, an orientation is required for the formation of cyclic duplexes, this H-bond prevents the formation of duplexes connected by all four base pairs. However, the central units of the UUA and AAU analogues **18** and **14** associate in CDCl₃/(D₆)DMSO 10:1 to form a cyclic duplex characterized by reverse *Hoogsteen* base pairing. The UUA tetramer **8** forms a cyclic UU homoduplex, while the AAU tetramer **21** forms only linear associates. Duplex formation of the *O*-silylated UUA and AAU tetramers is no longer prevented. The self-complementary UUA tetramer **22** forms *Watson–Crick*- and *Hoogsteen*-type base-paired cyclic duplexes more readily than the sequence-isomeric AAU tetramer **23**, further illustrating the sequence selectivity of duplex formation.

Introduction. – In pursuing the search for backbone-base integrating oligonucleotide analogues that pair by H-bonding and base stacking, we have analyzed partially protected, self-complementary dimers with an ethynylene linker between C(5') and either C(6) of uridine or C(8) of adenosine [1]. Such dimers, illustrated by the U*[c_y]A^(*) and A*[c_y]U^(*) ribonucleosides²⁾ **1** and **2**, associate in CHCl₃ solution by base pairing and, in part, by base stacking. They form either linear duplexes and higher associates, or cyclic duplexes. The type of association depends on the sequence, on the substituents at C(5'), C(6), and C(8) of unit I, on the configuration of C(5'), and on the substituent at C(5') of the adenine moiety II (R² = H or SiⁱPr₃) in the A*[c_y]U^(*) dimers **2**. The formation of cyclic duplexes requires a *syn*-conformation of unit I and a *gg*-type orientation of its ethynyl substituent at C(5'). This *gg*-orientation is prevented, in

¹⁾ Part 13: [1].

²⁾ *Conventions for abbreviated notation:* The substitution at C(6) of pyrimidines and C(8) of purines is denoted by an asterisk (*); for example U* and A* for hydroxymethylated uridine and adenosine derivatives. U^(*) and A^(*) represents both unsubstituted and hydroxymethylated nucleobases. The moiety linking C(6)–CH₂ or C(8)–CH₂ to C(5') of the adjacent unit is indicated in square brackets, such as [c] for a C-atom. The indices y, e, and a indicate a triple, double, or single bond, respectively.

$U^*[c_y]A^{(*)}$ dimers **1** ($X = OH$), by a persistent intramolecular H-bond from the propargylic $C(5')OH$ group to $N(3)$ of the adenine moiety [1–3], and this independently of the configuration at $C(5')$. Hence, $U^*[c_y]A^{(*)}$ dimers possessing a propargylic OH group form only linear duplexes and higher associates. Protection, or reductive removal of their propargylic OH group, as in the $U^*[c_y]A^{(*)}$ deoxy analogues **1a** and **1b**, allows the ethynyl moiety to adopt a *gg*-orientation, and leads to the formation of cyclic duplexes, particularly when the *syn*-conformation of unit I is favoured by a $C(8)$ substituent.



In contradistinction to the propargylic OH group of $U^*[c_y]A^{(*)}$ dimers **1**, the propargylic OH group of $A^*[c_y]U^{(*)}$ dimers **2** ($X = OH$) forms only a weakly persistent intramolecular H-bond to $O=C(2)$ of the uracil moiety, and may form an intermolecular H-bond in cyclic duplexes. The configuration of $C(5')$ of the $A^*[c_y]U^{(*)}$ dimers plays a greater role in determining the nature of the associates than for the $U^*[c_y]A^{(*)}$ sequence. A substituent at $C(6)$ favours the *syn*-conformation of the uracil moiety and the formation of cyclic duplexes. Depending on the configuration at $C(5')$, the nature of the substituent at $C(5')$, and the substitution of $C(6/I)$, $A^*[c_y]U^{(*)}$ dimers form either linear associates, or cyclic, more or less strongly associating dimers. These factors and the type of association of the $A^*[c_y]U^{(*)}$ and $U^*[c_y]A^{(*)}$ dimers **1** and **2** have been analyzed in detail [1].

The different persistence of the H-bond of the propargylic OH group in the $U^*[c_y]A^{(*)}$ and $A^*[c_y]U^{(*)}$ dimers is of crucial relevance for the ability of this type of dinucleoside analogues to form cyclic duplexes. To predict the ability of longer oligonucleosides to form duplexes, one must know how the factors governing the association of dimers operate in higher oligomers. We expected the H-bonds of the propargylic OH groups to affect the association of longer oligomers similarly as in

dimers, and probably in an additive way. To check the validity of this expectation, we planned to synthesize the four self-complementary $U^*[c_y]U^*[c_y]A^*[c_y]A$, $A^*[c_y]A^*[c_y]U^*[c_y]U$, $U^*[c_y]A^*[c_y]U^*[c_y]A$, and $A^*[c_y]U^*[c_y]A^*[c_y]U$ tetramers, and to analyze their association in comparison to the one of the two known self-complementary tetrameric $U^*[c_y]U^*[c_y]A^*[c_y]A$ and $A^*[c_y]A^*[c_y]U^*[c_y]U$ silyl ethers [4]. Protection of the propargylic OH group should remove the main obstacle to the formation of cyclic duplexes, while the association of the corresponding alcohols should be weakened in proportion to the number of $U^*[c_y]A^{(*)}$ and $A^*[c_y]A^{(*)}$ sequences and to their position. Such sequences should disfavour the formation of cyclic duplexes more strongly when they are in a central rather than in a peripheral position, as in the $U^*[c_y]U^*[c_y]A^*[c_y]A$ and $A^*[c_y]U^*[c_y]A^*[c_y]U$ tetramers. In contradistinction, the weakly persistent H-bond of the propargylic OH group of the uridine moieties may favour the formation of cyclic duplexes.

Results and Discussion. – 1. *Synthesis of the Tetrameric Triols.* The self-complementary tetramers **8**, **14**, **18**, and **21** were obtained by a linear synthesis based on the *Sonogashira* coupling of mono-, di-, and trimeric alkynes with 6-iodouridines and 8-iodoadenosines possessing a (trialkylsilyl)ethynyl group at C(5'), followed by desilylation of the coupling products.

The synthesis of the $U^*[c_y]U^*[c_y]A^*[c_y]A$ tetramer **8** began with a *Sonogashira* coupling of the dimer **5** with the *D-allo*-configured 6-iodouridine **3** [5] resulting from the desilylation of the known dimer **4** [2]. The coupling product was desilylated with Bu_4NF (TBAF) in THF to yield 45% of the *O*-isopropylidene protected $U^*[c_y]U^*[c_y]A$ trimer **6** (*Scheme 1*). A similar *Sonogashira* coupling of **6** with the 6-iodouridine **7** [5] gave the tetramer **8** in 34% yield.

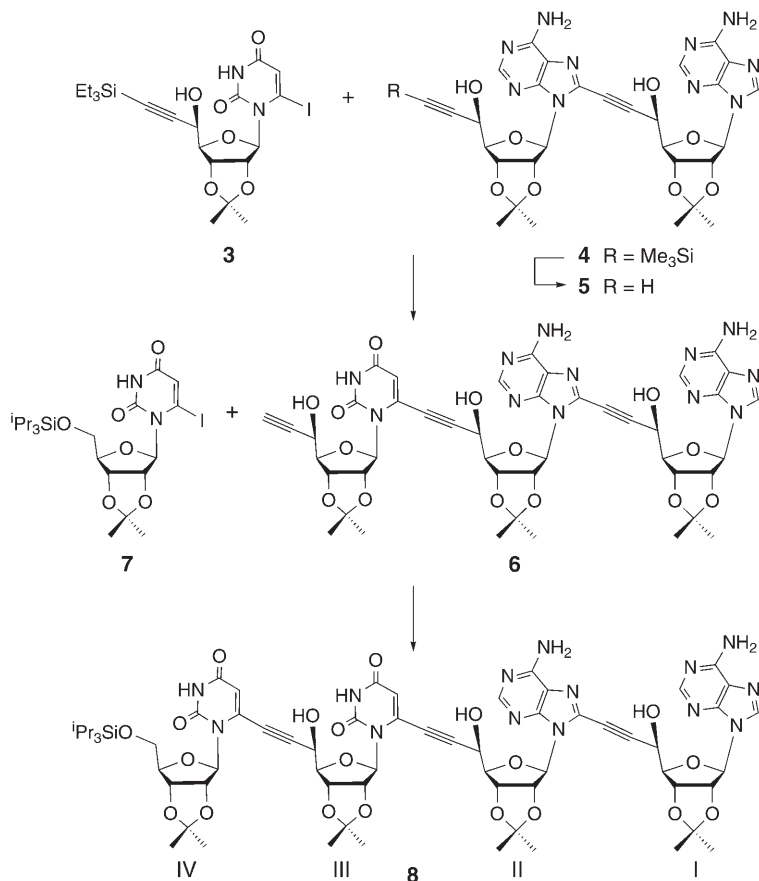
Similarly, the $A^*[c_y]A^*[c_y]U^*[c_y]U$ tetramer **14** was obtained from the 6-iodouridine **3** (*Scheme 2*). Coupling **3** and the alkyne **9** [5], followed by desilylation, yielded 63% of the $U^*[c_y]U$ dimer **10** that was coupled with the alkynylated 8-iodoadenosine **11** [2]. Desilylation of the coupling product afforded 41% of the $A^*[c_y]U^*[c_y]U$ trimer **12** that was coupled with the iodoadenosine **13** [1] to yield the tetramer **14** (57%).

To obtain the $U^*[c_y]A^*[c_y]U^*[c_y]A$ tetramer **18**, we coupled the alkyne **15** [2] with the iodouridine **3** (*Scheme 3*). Desilylation of the product yielded 37% of the $U^*[c_y]A$ dimer **16** that was coupled with the iodide **11**, followed by desilylation, to yield 55% of the $A^*[c_y]U^*[c_y]A$ trimer **17**. *Sonogashira* coupling of **17** with the iodouridine **7** gave the tetramer **18** (50%).

Finally, to prepare the $A^*[c_y]U^*[c_y]A^*[c_y]U$ tetramer **21**, we coupled the iodoadenosine **11** with the uridine-derived alkyne **9** (*Scheme 4*). Desilylation of the coupling product yielded 72% of the $A^*[c_y]U$ dimer **19**. The $U^*[c_y]A^*[c_y]U$ trimer **20** was similarly obtained in a yield of 70% by coupling **19** with **3**, followed by desilylation. The $A^*[c_y]U^*[c_y]A^*[c_y]U$ tetramer **21** was synthesized by coupling **20** with the 8-iodoadenosine **13** (61%).

2. *Fully Solvated Simplexes of the Tetrameric Triols 8, 14, 18, and 21 in (D₆)DMSO.* The analysis of the duplex formation of the tetramers requires detailed information of the spectroscopic data of the corresponding simplexes. ¹H- and ¹³C-NMR spectra were recorded of (D₆)DMSO solutions of the di-, tri-, and tetramers **5**, **6**, **8**, **10**, **12**, **14**, and **16–21**, and of the corresponding monomers **3**, **9**, **11**, and **15**. Selected chemical shifts

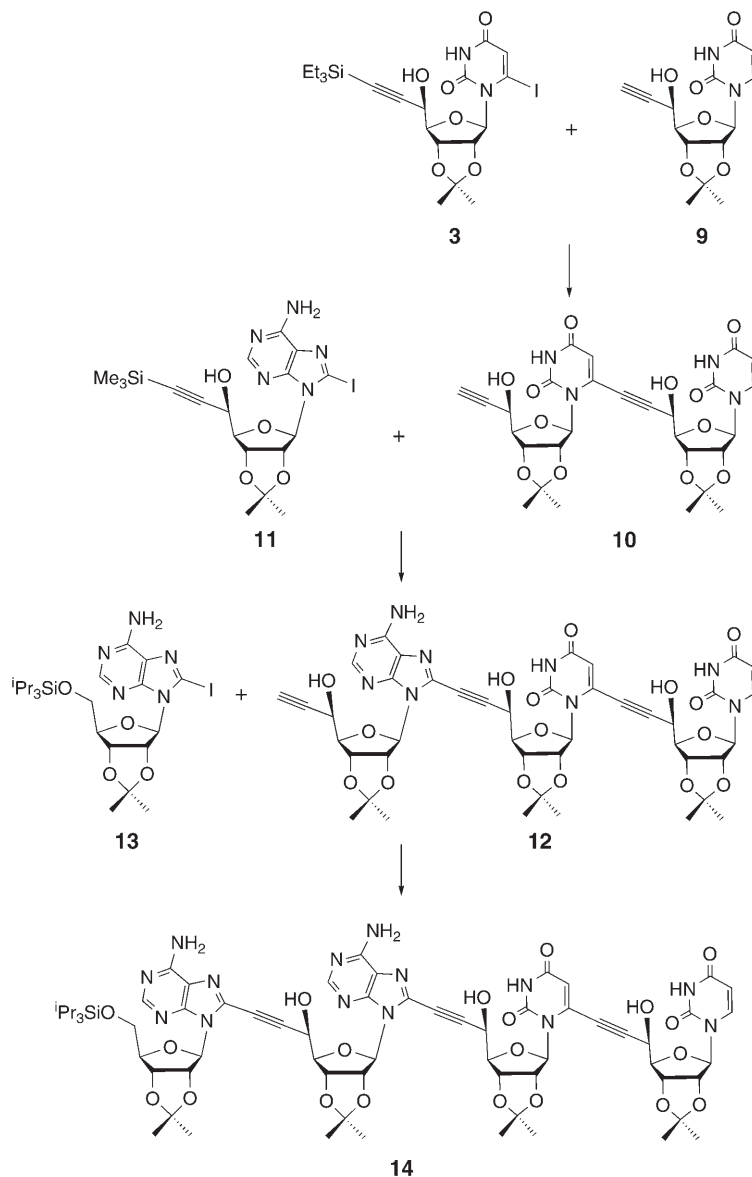
Scheme 1



and coupling constants are listed in *Tables 4–10* in the *Exper. Part*. As expected, the mono-, di-, tri-, and tetramers **3**, **5**, **6–12**, and **14–21** are molecularly dispersed in (D₆)DMSO, as evidenced by the values of the chemical shift for HN(3) and H₂N–C(6), and of the vicinal *J*(4',5') coupling.

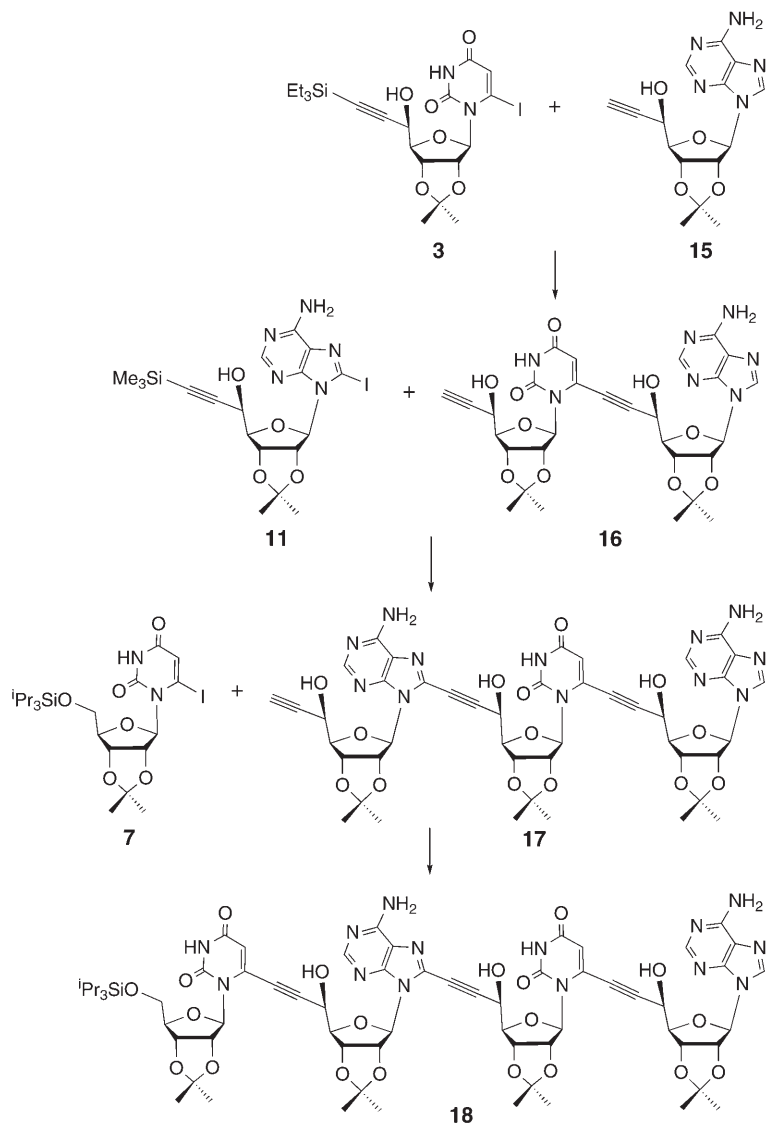
As described in the preceding publication (*Part 13*; [1]), the chemical shift of HN(3) and its concentration dependence are useful parameters to characterize the H-bonds involved in the association of ONIBs, and the effect of the substituent at C(6) of uridine (U) units. Indeed, HN(3) of unit I of the 6-unsubstituted mono- to tetramers resonates at 11.41–11.46 ppm, whereas substitution at C(6) leads to a downfield shift of *ca.* 0.25 ppm, with HN(3) of units II–IV of the di- to tetramers and of the 6-iodinated monomer **3** resonating at 11.61–11.71 ppm. One observes a similar effect of substitution at C(8) of adenosine (A) units on the chemical shift of H₂N–C(6). H₂N–C(6) of the unit I_A (8-unsubstituted) of mono- to tetramers resonates at 7.34–7.38 ppm, whereas H₂N–C(6) of units II_A* and III_A* of di- to tetramers resonates at

Scheme 2



7.62–7.68 ppm, and H₂N–C(6) of the 8-iodinated monomer **11** at 7.56 ppm. Thus, substitution at C(8) by an ethynyl or iodo group leads to a downfield shift of *ca.* 0.30 and 0.20 ppm, respectively. H₂N–C(6) of unit IV_{A*} of the tetramers **14** and **21**, however, resonates at 7.52–7.53 ppm. This difference is due to the effect of the partially persistent intramolecular O(5'/II–III)–H ⋯ N(3/II–III) H-bond, resulting in a

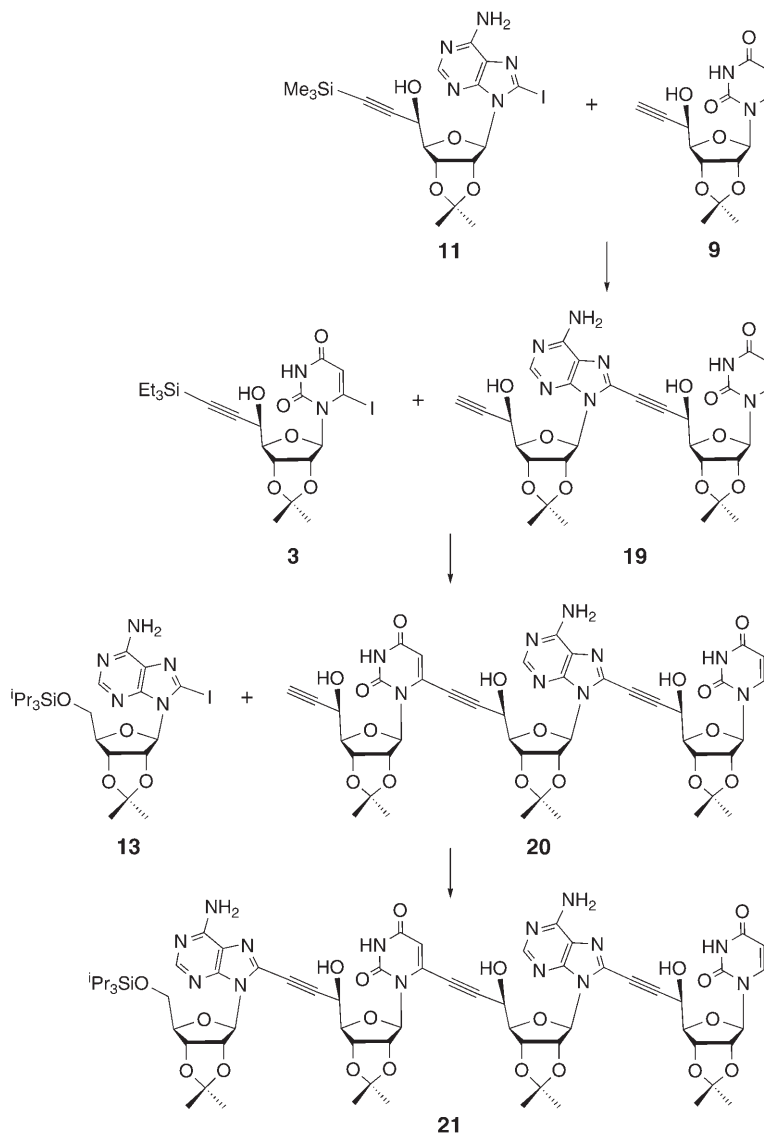
Scheme 3



downfield shift of *ca.* 0.15 ppm for $\text{H}_2\text{N}-\text{C}(6/\text{II}-\text{III})$ that is added to the similar downfield shift resulting from alkylation at C(8).

Weak intramolecular H-bonds are broken by changing the solvent from CHCl_3 to DMSO, whereas strong ones may partially survive (see [6] and refs. cit. therein). The intramolecular $\text{O}-\text{H} \cdots \text{N}(3)$ H-bonds of $\text{A}^*[\text{c}_y]\text{A}$ diols in (D_6) DMSO were indeed replaced to an extent of 80% (unit I) and 40–50% (unit II) by H-bonds to the solvent [2]. The weak intramolecular $\text{O}-\text{H} \cdots \text{O}=\text{C}(2)$ in uridine units should be completely

Scheme 4



replaced by H-bonds to DMSO. This was found to be the case, as $J(5',\text{OH}) = 5.7$ Hz of the 6-unsubstituted uridine **9** evidences a completely solvated OH group (see *Table 4* in the *Exper. Part*). By comparison, $J(5,\text{OH})$ of *D-allo*-configured adenosine-derived propargyl alcohols possessing a completely persistent intramolecular H-bond is small (≤ 1.5 Hz [2][3]). $J(5',\text{OH}) = 5.1$ Hz of the 8-unsubstituted adenosine **15** is slightly smaller than the one of **9**, and indicates a *ca.* 15% persistence of the intramolecular

C(5')OH...N(3) H-bond. This interpretation is supported by the downfield shift for HO–C(5') of **15** as compared to that of **9** (6.29 vs. 6.08 ppm). The effect of uracylation and adeninylation, enhancing the acidity of the propargyl alcohols [1], is clearly seen by comparing the chemical shift of HO–C(5') of A and A* units in the different positions of dimers to tetramers, and, similarly, of HO–C(5') of U and U* units. HO–C(5'/I_A) of the di- to tetramers **5**, **6**, **8**, and **16–18** resonates downfield at 6.67–6.72 ppm, HO–C(5'/II_A) of **6**, **8**, **20**, and **21** at 6.71–6.74 ppm, and HO–C(5'/III_A) of **14** and **18** at 6.78–6.79 ppm. Similarly, HO–C(5'/I_U) of **10**, **12**, **14**, and **19–21** resonates at 6.50–6.55 ppm, and HO–C(5'/II_U or III_U) of **8**, **12**, **14**, **17**, **18**, and **21** at 6.36–6.38 ppm (see *Tables 5, 7, and 9* in the *Exper. Part*). The di- and trimers possess an unsubstituted terminal ethynyl group, and the absence of a nucleobase substituent is reflected by the upfield shift of HO–C(5'/II_A or III_A) of **5**, **19**, **12**, and **17**, resonating at 6.35–6.40 ppm, and of HO–C(5'/II_U or III_U) of **10**, **16**, **6**, and **20**, resonating at 5.81–5.83 ppm. *J*(5',OH) of the uridine units of all these di- to tetramers is larger than *J*(5',OH) of the adenosine units (5.9–7.0 vs. 4.9–6.0 Hz), again evidencing a *ca.* 15% persistence of the intramolecular H-bond in the adenosine units.

The chemical shift for H–C(2') is characteristic of *anti*- and *syn*-conformers of 2,3-*O*-isopropylidened and 5'-*O*-protected uridines (4.8–4.9 vs. 5.15–5.25 ppm) and adenosines (5.1–5.2 vs. 5.6–5.7 ppm) in CDCl₃ [1], and remains a valid parameter for solutions in (D₆)DMSO. This is evidenced by δ (H–C(2'_U)) of **9** (4.90 ppm), δ (H–C(2'/IV_U)) of **8** and **18** (5.16–5.20 ppm), δ (H–C(2'_A)) of the *N*⁶-benzoylated and 5'-*O*-triethylsilylated derivative of **15** [7] (5.12 ppm³), and δ (H–C(2'/IV_A)) of **14** and **21** (5.60–5.61 ppm; see *Tables 4 and 9* in the *Exper. Part*). Intra- and intermolecular H-bonding of HO–C(5') of the adenosine, but not of the uridine units leads to an upfield shift for H–C(2') (typically 5.20 ppm for a completely persistent intramolecular H-bond in CDCl₃ [1][3]). Indeed, H–C(2'/II_A) of **5**, **6**, **8**, and **19–21**, and H–C(2'/III_A) of **12**, **14**, **17**, and **18** resonate upfield by *ca.* 0.2 ppm at 5.40–5.50 ppm, whereas H–C(2'/II_U) of **10**, **12**, **14**, and **16–18**, and H–C(2'/III_U) of **6**, **8**, **20**, and **21** resonate at 5.16–5.26 ppm and do not show an upfield shift (see *Tables 5, 7, and 9* in the *Exper. Part*). Upfield shifts for H–C(2'/I_A) and H–C(2'/I_U) relative to H–C(2'/II_A) and H–C(2'/II_U) evidence a (partial) population of the *anti*-conformation. A weak upfield shift of *ca.* 0.05 ppm is observed for H–C(2'/I_A) of **5**, **6**, **8**, and **16–18**, and a stronger one of *ca.* 0.20 ppm for H–C(2'/I_U) of **10**, **12**, **14**, and **19–21**, evidencing a minor contribution of the *anti*-conformer in the I_A series and a 3:2 *anti/syn* equilibrium in the I_U series. In both series, the *anti*-conformers of unit I are less favoured in the di- to tetramers than in the corresponding monomers, as evidenced by δ (H–C(2')) values of 5.30 and 4.90 ppm for **15** and **9**, respectively.

The *syn/anti*-equilibrium of the di- to tetramers is also correlated with the C(4',5') conformation, as reflected by *J*(4',5'). A *syn*-oriented uracil moiety is sterically more demanding than a *syn*-oriented adenine moiety, resulting in a stronger preference of the

³) 2,3-*O*-Isopropylidened and 5'-*O*-protected adenosines adopt an *anti*-conformation in CDCl₃. In (D₆)DMSO, these nucleosides populate a *syn*-conformation to an extent that increases as the size of the substituent at C(4') gets smaller. This is illustrated by the downfield shift for H–C(2') in the adenosine series that increases, as R at C(4') changes from CH(OSiEt₃)C≡CH (5.12 ppm) to CH₂OTr (5.45 ppm [8]), CH₂OCO₂Ph (5.50 ppm [9]), and CH₂OBz (5.53 ppm [10]).

tg-conformer (H–C(4') and H–C(5') antiperiplanar). Indeed, $J(4',5'/\Pi_U)$ and $J(4',5'/\text{III}_U)$ values of the di- to tetramers **6**, **8**, **10**, **12**, **14**, **16**–**18**, **20**, and **21** are distinctly larger than $J(4',5'/\text{II}_A)$ and $J(4',5'/\text{III}_A)$ values of **5**, **6**, **8**, **12**, **14**, and **17**–**21** (8.8–9.1 Hz vs. 6.4–7.5 Hz; see *Tables 5*, *7*, and *9* in the *Exper. Part*). The 3 : 2 *anti/syn*-equilibrium for the I_U units of **10**, **12**, **14**, and **19**–**21** correlates with a strong decrease of the $J(4',5'/\text{I}_U)$ values from 8.8–9.1 to 6.2–6.6 Hz, whereas the minor contribution of the *anti*-conformer in the *syn/anti*-equilibrium for the I_A units of **5**, **6**, **8**, and **16**–**18** leads to only a slight decrease of the $J(4',5'/\text{I}_A)$ values from 6.4–7.5 to 5.7–6.3 Hz. The (*N*)-conformation is more strongly preferred by the uridine moieties of units II–IV of di- to tetramers than of unit I ($J(1',2')/J(3',4') = 0.25$ – 0.75 and 0.45 – 1.25), whereas the adenosine moieties of units I–IV adopt a *ca.* 1 : 1 (*N*)/(*S*)-equilibrium ($J(1',2')/J(3',4') = 0.6$ – 1.6).

The ^{13}C -NMR spectra of the di- to tetramers show the characteristic chemical shifts for uracylated, adenylated, and monosubstituted ethynyl moieties (101.2–102.5/73.4–75.2, 95.1–96.8/72.6–74.4, and 83.0–84.7/74.8–75.9 ppm, resp.; see *Tables 6*, *8*, and *10* in the *Exper. Part*).

3. Duplex Formation of the Tetrameric Triols **8, **14**, **18**, and **21** in $\text{CDCl}_3/(\text{D}_6)\text{DMSO } 10 : 1$.** As the tetramers **8**, **14**, **18**, and **21** are poorly soluble in CDCl_3 , we investigated their association in $\text{CDCl}_3/(\text{D}_6)\text{DMSO } 10 : 1$. The strongly persistent intramolecular H-bond to N(3) of the adenosine units is expected to prevent the formation of cyclic duplexes connected by all four base pairs, and should thus play a decisive role in determining the association. One expects the central units of the $\text{U}^*[\text{c}_y]\text{A}^*[\text{c}_y]\text{U}^*[\text{c}_y]\text{A}$ tetramer **18** to form a cyclic AU heteroduplex with a stability differing from the one formed by the central units of the $\text{A}^*[\text{c}_y]\text{A}^*[\text{c}_y]\text{U}^*[\text{c}_y]\text{U}$ tetramer **14**; the analysis discussed below showed that the one formed by **18** is more stable. It also showed that the uridine units of the $\text{U}^*[\text{c}_y]\text{U}^*[\text{c}_y]\text{A}^*[\text{c}_y]\text{A}$ tetramer **8** are involved in a cyclic UU homoduplex, and that, not surprisingly, the $\text{A}^*[\text{c}_y]\text{U}^*[\text{c}_y]\text{A}^*[\text{c}_y]\text{U}$ tetramer **21** does not form any cyclic duplex.

Considering the decisive effect on duplex formation of intramolecular vs. intermolecular H-bonds, and the effect of DMSO on H-bonding, we began the analysis by determining the effects of the solvent, comparing the ^1H -NMR spectra of the uridine and adenosine monomers **9** and **15** in CDCl_3 and $\text{CDCl}_3/(\text{D}_6)\text{DMSO } 10 : 1$ (see *Table 4* in the *Exper. Part*).

Addition of 10% (D_6)DMSO to CDCl_3 leads to a weak upfield shift for HO–C(5') of the adenosine **15** from 7.76 to 7.41 ppm and to a slight increase of the $J(5',\text{OH})$ value from 1.8 to 2.4 Hz. This evidences a *ca.* 90% persistence of the intramolecular H-bond to N(3) that is also evidenced by the small $J(4',5')$ value of 2.1 Hz and by the (*S*)-conformation ($J(1',2')/J(3',4') = 2.3$). The shift for H–C(2') of the uridine **9** in CDCl_3 (5.00 ppm) reveals a *ca.* 1 : 2 *syn/anti*-equilibrium. The shift of HO–C(5') (3.23 ppm) and $J(5',\text{OH}) = 3.0$ Hz agree with an intramolecular H-bond to O–C(4') whereof *ca.* 30% are involved in a bifurcated H-bond to O=C(2). In $\text{CDCl}_3/(\text{D}_6)\text{DMSO } 10 : 1$, the upfield shift of H–C(2') (4.57 ppm) evidences the *anti*-conformation, and $J(5',\text{OH}) = 4.5$ Hz (as compared with 5.7 Hz in pure (D_6)DMSO) a *ca.* 50% persistence of the H-bond to O–C(4'). Surprisingly, adding 10% (D_6)DMSO to CDCl_3 induces an upfield shift for H–C(2') of **9** (4.57 vs. expected 4.8–4.9 ppm for CDCl_3 and (D_6)DMSO solutions) and **15** (4.95 vs. expected 5.2–5.3 ppm); this effect may be general for

solutions in $\text{CDCl}_3/(\text{D}_6)\text{DMSO}$ 9:1 and has to be taken into account in analysing the association of the tetramers. $\text{HN}(3)$ of **9** and $\text{H}_2\text{N}-\text{C}(6)$ of **15** resonate in $\text{CDCl}_3/(\text{D}_6)\text{DMSO}$ 9:1 at 10.6 and 6.2 ppm, respectively. Ethynylation of the nucleobases is expected to lead to a similar additional downfield shift for $\text{HN}(3)$ and $\text{H}_2\text{N}-\text{C}(6)$ as observed for solutions in pure $(\text{D}_6)\text{DMSO}$ (0.25 and 0.3 ppm, resp., see above).

The formation of tetramer duplexes connected by all four AU base pairs is only possible by breaking the intramolecular $\text{O}-\text{H} \cdots \text{N}(3/\text{I}-\text{III})$ H-bonds. The persistence of these H-bonds was determined by analyzing the $^1\text{H-NMR}$ spectra of the tetramers **8**, **14**, **18**, and **21**. The tetramers **8**, **18**, and **21** show well-resolved spectra for 0.5–11 mM solutions in $\text{CDCl}_3/(\text{D}_6)\text{DMSO}$ 10:1, whereas the $\text{A}^*[\text{c}_y]\text{A}^*[\text{c}_y]\text{U}^*[\text{c}_y]\text{U}$ tetramer **14** shows broad signals at ambient temperature over the whole concentration range, preventing an exact analysis, particularly of the coupling constants. Chemical-shift values and coupling constants for 10–11 and 1 mM solutions of **8**, **18**, and **21** are listed in Table 1. For 10–11 mM solutions, the strong downfield shift of $\text{HO}-\text{C}(5'/\text{I}_\text{A})$ of **8** and **18** (7.40 and 7.36 ppm), $\text{HO}-\text{C}(5'/\text{II}_\text{A})$ of **8** and **21** (7.58 and 7.74 ppm), and $\text{HO}-\text{C}(5'/\text{III}_\text{A})$ of **18** (7.74 ppm), and the small $J(4',5')$ and $J(5',\text{OH})$ values of the adenosine units of **8**, **18**, and **21** (≤ 1.8 Hz) evidence completely persistent $\text{O}-\text{H} \cdots \text{N}(3/\text{I}-\text{III})$ H-bonds. Hence, these tetramers cannot form duplexes connected by four AU base pairs, while cyclic heteroduplexes connected by two AU base pairs are possible for **14**, **18**, and **21** (Fig. 1). The $\text{U}^*[\text{c}_y]\text{U}^*[\text{c}_y]\text{A}^*[\text{c}_y]\text{A}$ tetramer **8** cannot form a cyclic heteroduplex.

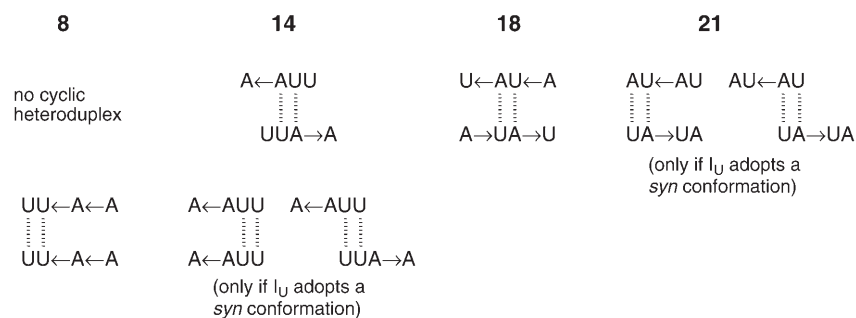


Fig. 1. Possible cyclic AU and UU duplexes of the tetramers **8**, **14**, **18**, and **21** possessing completely persistent intramolecular H-bonds to $\text{N}(3)$ of the adenine units (the arrows indicate these H-bonds and the *tg*-orientation of the ethynyl moiety)

$\text{HO}-\text{C}(5'/\text{I}-\text{III})$ of the uridine units of **8**, **18**, and **21** (10–11 mM solutions) are more or less completely solvated, as evidenced by $\delta(\text{OH})$ of 5.44–5.88 ppm and $J(5',\text{OH})$ of 5.1–5.7 Hz. The $\text{A}^*[\text{c}_y]\text{U}^*[\text{c}_y]\text{A}^*[\text{c}_y]\text{U}$ tetramer **21** forms only linear duplexes. This is evidenced by the antiperiplanar $\text{H}-\text{C}(4')$ and $\text{H}-\text{C}(5')$ of units I and III ($J(4',5'/\text{I})$ and $J(4',5'/\text{III})$ of 8.7–9.0 Hz), and corroborated by a small effect of the concentration on the chemical shift of the $\text{H}-\text{C}$ signals, observed upon dilution to 1 mM ($\Delta\delta \leq 0.05$ ppm; with the exception of 0.10–0.13 ppm for $\text{H}-\text{C}(2/\text{IV})$ and $\text{H}-\text{C}(1'/\text{IV})$).

The $J(4',5'/\text{II})$ value of the $\text{U}^*[\text{c}_y]\text{A}^*[\text{c}_y]\text{U}^*[\text{c}_y]\text{A}$ tetramer **18** increases from 4.8 to 6.9 Hz upon dilution from 10 to 1 mM. These values agree well with those of the cyclic

duplexes of $A^*[c_y]U^*$ dimers ($J(4',5'/I) \approx 6$ Hz [1]), and evidence that the central units of **18** form a cyclic heteroduplex.

The $J(4',5'/III_U)$ value of **8** (6.9 Hz) is distinctly smaller than $J(4',5'/I_U)$ and $J(4',5'/III_U)$ values of **21** ($\Delta J \approx 2$ Hz), suggesting a (minor) contribution of a cyclic duplex. As discussed above, **8** cannot form a cyclic heteroduplex, so that the cyclic duplex can only be a homoduplex involving two UU base pairs.

The 1H -NMR signals of a 10 mM solution of the $A^*[c_y]A^*[c_y]U^*[c_y]U$ tetramer **14** in $CDCl_3$ become sharper as the temperature is increased. At 50° , the $H-C(4')$ signals are well resolved. $H-C(4'/III)$ resonates at 4.42 ppm as a t ($J(3',4'/III) \approx J(4',5'/III) \approx 2.0$ Hz) and $H-C(4'/II)$ as a dd at 4.05 ppm ($J(3',4'/II) = 4.8$, $J(4',5'/III) = 5.7$ Hz), whereas the signals of $H-C(4'/I)$ and $H-C(4'/IV)$ overlap at 4.11–4.17 ppm. The $J(4',5'/II)$ value agrees with the formation of cyclic duplexes of the central units.

The different duplexes of **8**, **14**, **18**, and **21** are also reflected by the chemical-shift values for $HN(3)$ (Table 1). For 10–11 mM solutions, $HN(3/II)$ of **18**, engaged in a cyclic heteroduplex, resonates at lowest field (11.83 ppm), followed by $HN(3/IV)$ of **8** engaged in a cyclic homoduplex (11.40 ppm). $HN(3/IV)$ of **18**, $HN(3/I)$ of **21**, $HN(3/III)$ of **21**, and $HN(3/III)$ of **8** resonate at 11.25–11.33 ppm, and are only involved in linear duplexes. $HN(3/I)$ and $HN(3/II)$ of **14** resonate as a broad s at 11.5–10.8 ppm at ambient temperature and as two broad ss at 11.7–11.3 and 11.1–10.8 ppm at 50° . This evidences that $HN(3/II)$ of **14** is involved in a cyclic duplex.

The concentration dependence of the chemical shift of selected $HN(3)$ of **8**, **18**, and **21** (11 to 1 mM solutions) is shown in Fig. 2. The tetramers **18** and **8** show two $HN(3)$ signals over the whole concentration range. As the signal of $HN(3/IV)$ of **8** is broad, its temperature dependence is not depicted in Fig. 2. $HN(3/I)$ and $HN(3/III)$ of **21** give rise to a single signal at high concentrations and to two signals at low concentration; one of the signals shows no concentration dependence and the other, tentatively assigned to $HN(3/III)$, a weak one ($\Delta\delta_{\max} = 0.13$ ppm). The curves in Fig. 2 do not flatten out at high concentration. The curve progression, and the small downfield shift for $HN(3/IV)$ of **18**, $HN(3/I)$ of **21**, and $HN(3/III)$ of **8** evidence an equilibrium of simplex (expected $\delta(HN(3)) = 10.8$ – 10.9 ppm), linear duplexes, and at best small amounts of higher associates. The larger downfield shift for $HN(3/II)$ of **18** evidences an equilibrium of simplex, linear and cyclic duplexes, and small amounts of higher associates. The type of pairing in cyclic duplexes of $A^*[c_y]U^{(*)}$ dimers in $CDCl_3$ is reflected by the chemical shift of $HN(3)$ (11.5–11.9 ppm for reverse *Hoogsteen* base pairing and 12.3–12.8 ppm for *Watson–Crick* base pairing [1]). Insofar as this may be extrapolated to the cyclic duplexes of **18** in $CDCl_3/(D_6)DMSO$ 10:1, the chemical shift for $HN(3/II)$ of a 12.5 mM solution of **18** (11.84 ppm) evidences a reverse *Hoogsteen* base-paired duplex. This duplex is favoured by an intermolecular H-bond of $HO-C(5'/II)$ to $O=C(4/II)$ and by a cooperativity between the intramolecular H-bond of $HO-C(5'/III)$ to $N(3/III)$ and intermolecular H-bonds from $H_2N-C(6/III)$ [1].

The temperature dependence of $\delta(HN(3))$ of 3 mM solutions of **8**, **18**, and **21** was determined from 0 to 50° in 10° steps. However, graphical analysis [11] or analysis by linear least-squares fitting [12] did not lead to reliable thermodynamic parameters.

CD Spectra of 0.2 mM solutions of **8**, **14**, **18**, and **21** were recorded at -10 to 50° in 10° steps (Fig. 3). Only the CD spectrum of **18** shows a strong temperature dependence, evidencing π -stacking in a cyclic duplex; the strong absorption is in

Table 1. Selected $^1\text{H-NMR}$ Chemical Shifts [ppm] and Coupling Constants [Hz] for 10–11 mM and, in Parentheses, for 1 mM Solutions of the Tetramers **8**, **18**, and **21** in $\text{CDCl}_3/(D_6)\text{DMSO}$ 10:1 at 20 $^\circ\text{C}$ ^{a)}

Sequence	8 UUA A	18 UAUA	21 AU AU
H–C(5/I) or H–C(2/I)	8.04 (8.05)	8.05 (8.06)	5.49 (5.48)
H–C(6/I) or H–C(8/I)	7.83 (7.81)	7.83 (7.81)	7.68 (7.63)
HN(3/I) or H ₂ N–C(6/I)	6.42 (6.26)	6.52 (6.29)	11.27 (11.15)
H–C(1'/I)	5.86 (5.84)	5.84 (5.83)	5.94 (5.885)
H–C(2'/I)	4.93–5.08	4.88–5.12	4.94–5.10
H–C(3'/I)	4.93–5.08	4.88–5.12	4.94–5.10
H–C(4'/I)	4.40 (4.41)	4.33 (4.34)	4.23 (4.19)
H–C(5'/I)	4.76 (4.77)	4.73 (4.75)	4.63 (4.63)
HO–C(5'/I)	7.40 (7.52)	7.36 (7.50)	5.70 (5.59)
H–C(5/II) or H–C(2/II)	8.03 (8.04)	5.69 (5.73)	8.05 (8.09)
HN(3/II) or H ₂ N–C(6/II)	6.72 (6.55)	11.83 (11.40) ^{b)}	^{d)}
H–C(1'/II)	6.07 (6.08)	5.98 (5.99)	5.87 (5.92)
H–C(2'/II)	4.93–5.08	4.88–5.12	4.94–5.10
H–C(3'/II)	4.93–5.08	4.88–5.12	4.94–5.10
H–C(4'/II)	4.32 (4.33)	4.02 (4.03)	4.18 (4.20)
H–C(5'/II)	4.76 (4.77)	4.65 (4.63)	4.72 (4.73)
HO–C(5'/II)	7.58 (7.62)	5.69 (5.44)	7.74 (7.73)
H–C(5/III) or H–C(2/III)	5.71 (5.73)	7.93 (8.01)	5.70 (5.71)
HN(3/III) or H ₂ N–C(6/III)	11.25 (11.05)	6.90 (6.59)	11.27 (11.25)
H–C(1'/III)	6.02 (6.03) ^{b)}	6.09 (6.11)	6.08 (6.10)
H–C(2'/III)	4.93–5.08	4.88–5.12	4.94–5.10
H–C(3'/III)	4.90 (4.91)	4.88–5.12	4.94–5.10
H–C(4'/III)	4.00 (4.01)	4.33 (4.34)	4.06 (4.09)
H–C(5'/III)	4.59 (4.58)	4.73 (4.75)	4.50 (4.53)
HO–C(5'/III)	5.44 (5.37)	7.74 (7.81)	5.88 (5.89)
H–C(5/IV) or H–C(2/IV)	5.76 (5.79)	5.69 (5.72)	8.23 (8.33)
HN(3/IV) or H ₂ N–C(6/IV)	11.40 (11.25)	11.33 (11.14) ^{b)}	^{d)}
H–C(1'/IV)	6.01 (6.02) ^{b)}	6.02 (6.03)	6.58 (6.45)
H–C(2'/IV)	4.93–5.08	4.88–5.12	5.43 (5.43)
H–C(3'/IV)	4.62 (4.63)	4.64 (4.64)	4.94–5.10
H–C(4'/IV)	3.93 (3.94)	3.95 (3.96)	4.06 (4.07)
H _a –C(5'/IV)	3.63 (3.64)	3.65 (3.66)	3.68 (3.68)
H _b –C(5'/IV)	3.63 (3.64)	3.65 (3.66)	3.54 (3.54)
$J(5,6/I)$	–	–	7.8 (8.1)
$J(1',2'/I)$	3.6 (3.0)	3.9 (3.9)	<1.0 (<1.0)
$J(2',3'/I)$	^{d)}	^{d)}	^{d)}
$J(3',4'/I)$	<1.5 (<1.0)	<1.5 (<1.5)	3.6 (3.6)
$J(4',5'/I)$	1.8 (2.4)	<1.5 (<1.5)	9.0 (8.4)
$J(5',\text{OH}/I)$	<1.5 (3.0)	<1.5 (1.5)	5.7 (5.7)
$J(1',2'/II)$	4.2 (4.5)	<1.0 (<1.0)	5.4 (5.4)
$J(2',3'/II)$	^{d)}	^{d)}	^{d)}
$J(3',4'/II)$	<1.5 (<1.0)	4.8 (3.6)	0 (<1.5)
$J(4',5'/II)$	1.8 (2.4)	4.8 (6.9)	1.2 (<1.5)
$J(5',\text{OH}/II)$	<1.5 (3.0)	^{d)} (5.1)	<1.5 (2.1)
$J(1',2'/III)$	1.5 (1.8) ^{c)}	4.8 (4.8)	<1.5 (1.5)
$J(2',3'/III)$	6.3 (6.3)	^{d)}	^{d)}
$J(3',4'/III)$	3.9 (3.9)	<1.5 (<1.5)	3.6 (3.3)
$J(4',5'/III)$	6.9 (7.2)	<1.5 (<1.5)	8.7 (8.1)
$J(5',\text{OH}/III)$	5.1 (5.1)	<1.5 (<1.5)	5.7 (5.7)
$J(1',2'/IV)$	1.5 (1.2) ^{c)}	<1.0 (1.2)	1.5 (1.5)
$J(2',3'/IV)$	6.3 (6.3)	^{d)} (6.0)	6.3 (6.3)
$J(3',4'/IV)$	4.2 (4.2)	4.5 (4.8)	^{d)}
$J(4',5'_a/IV)$	6.3 (6.3)	6.0 (6.6)	6.9 (6.9)
$J(4',5'_b/IV)$	6.3 (6.3)	6.0 (6.6)	6.9 (6.9)
$J(5'_a,5'_b/IV)$	^{d)}	^{d)}	10.2 (10.2)

^{a)} Assignments based on a DQF-COSY spectrum. ^{b)} ^{c)} Assignments may be interchanged. ^{d)} Not determined.

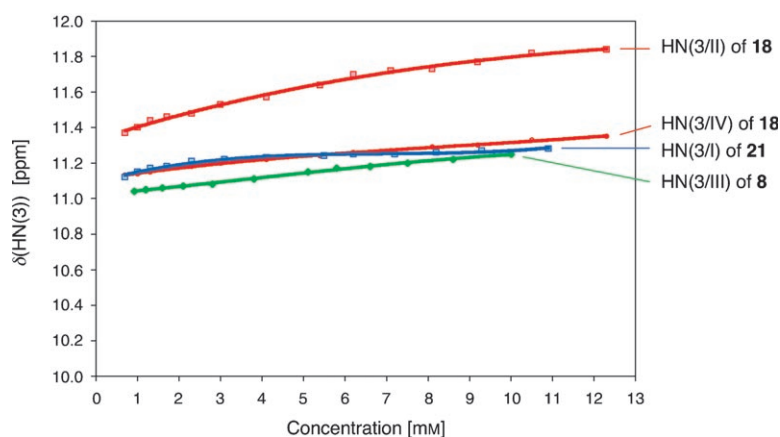


Fig. 2. Concentration dependence of $\delta(\text{HN}(3/\text{III}))$ of **8**, $\delta(\text{HN}(3/\text{I}))$ of **21**, and $\delta(\text{HN}(3/\text{II}))$ and $\delta(\text{HN}(3/\text{IV}))$ of **18** in $\text{CDCl}_3/(D_6)\text{DMSO } 10:1$

agreement with a reverse *Hoogsteen* base pairing (see [1]). The ROESY of **18** shows no cross-peak for the broad HN(3/II) signal, but this is no proof for a *Hoogsteen*-type base pairing, since the cross-peaks between the sharper signal of HN(3/IV) and both H–C(2/I) and H–C(8/I), expected for a partial formation of linear duplexes, were also missing. The weak temperature dependence of the CD spectra of **8** and **14** suggests that only small amounts of cyclic duplexes are formed at this (low) concentration.

That the $\text{U}^*[\text{c}_y]\text{A}^*[\text{c}_y]\text{U}^*[\text{c}_y]\text{A}$ tetramer **18** forms cyclic duplexes more readily than the $\text{A}^*[\text{c}_y]\text{A}^*[\text{c}_y]\text{U}^*[\text{c}_y]\text{U}$ tetramer **14** is surprising, as the tetramers differ only by the permutation of their peripheral units. The exclusive formation of linear duplexes and higher associates of **21** may be rationalized by an *anti*-conformation of the uracil moiety of unit I, but overlap of the H–C(2) and H–C(3) signals prevented an unambiguous assignment of this conformation.

As protection of the propargylic OH groups should allow the formation of cyclic duplexes connected by four base pairs, we investigated the duplex formation of the known, self-complementary $\text{U}^*[\text{c}_y]\text{U}^*[\text{c}_y]\text{A}^*[\text{c}_y]\text{A}$ and $\text{A}^*[\text{c}_y]\text{A}^*[\text{c}_y]\text{U}^*[\text{c}_y]\text{U}$ silyl ethers **22** and **23** [13] in CDCl_3 .

4. *Duplex Formation of the Tetrameric Silyl Ethers 22 and 23 in CDCl_3 .* The solution of the $\text{U}^*[\text{c}_y]\text{U}^*[\text{c}_y]\text{A}^*[\text{c}_y]\text{A}$ silyl ether **22** in CDCl_3 shows a higher proportion of cyclic duplexes than the solution of the $\text{A}^*[\text{c}_y]\text{A}^*[\text{c}_y]\text{U}^*[\text{c}_y]\text{U}$ isomer **23**. This is evidenced by the smaller $J(4',5')$ coupling constants of **22** and by the stronger change of the chemical shift of the CH signals of all units upon addition of 10% of CD_3OD . Large $J(4',5')$ values for solutions of both **22** and **23** in $\text{CDCl}_3/\text{CD}_3\text{OD } 10:1$ evidence a completely solvated simplex. Due to coalescence, the HN(3/III) and HN(3/IV) signals of **22** are not visible in the $^1\text{H-NMR}$ spectrum of a 10 mM solution in CDCl_3 recorded at 293–323 K. The appearance of three HN(3) signals at lower temperature evidences an equilibrium of cyclic duplexes connected by *Watson–Crick*- and *Hoogsteen*-type base pairing.

$^1\text{H-NMR}$ spectra were recorded of 10 mM solutions of **22** and **23** in CDCl_3 and in $\text{CDCl}_3/\text{CD}_3\text{OD } 9:1$ (Table 2; partly published in [13]). The unambiguous assignment

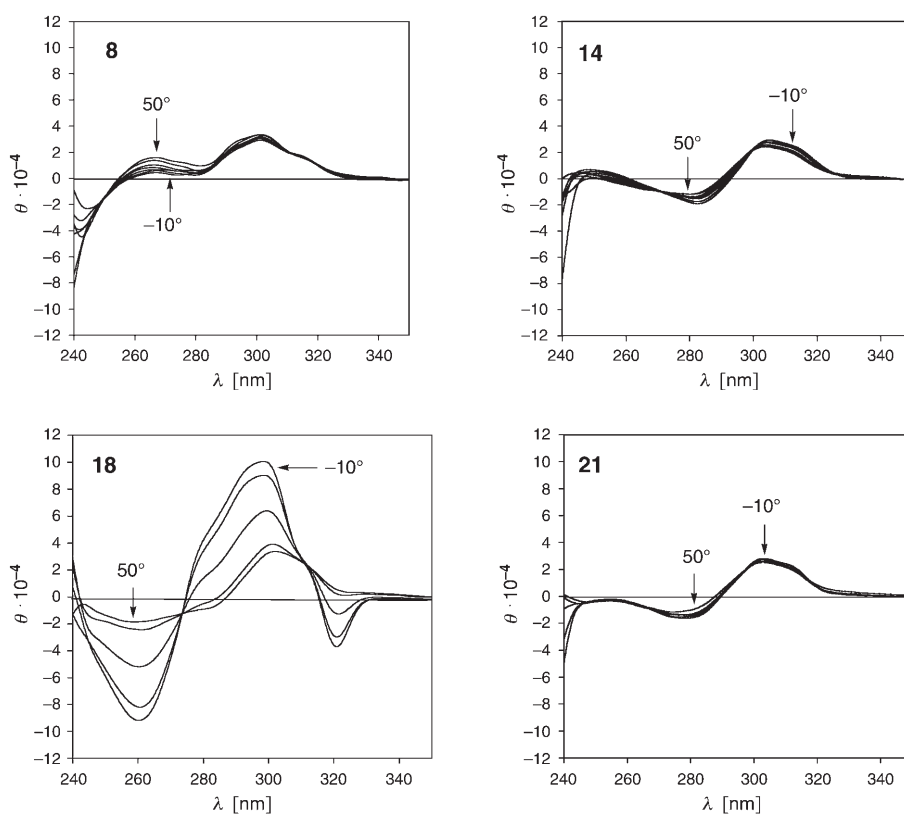


Fig. 3. CD Spectra for 0.2 mM solutions of the tetramers **8**, **14**, **18**, and **21** in $\text{CHCl}_3/\text{DMSO}$ 10:1 recorded at -10 to 50° in 10° steps

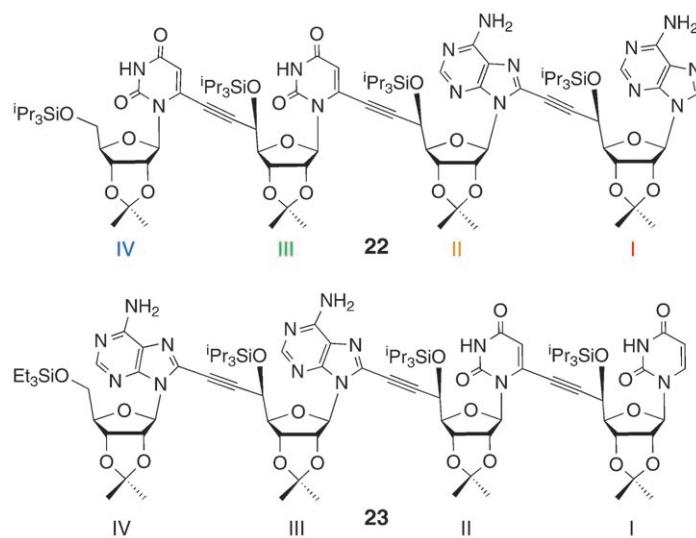


Table 2. Solvent Dependence of Selected ^1H -NMR Chemical Shifts [ppm] and Coupling Constants [Hz] of the Tetrameric Tripropargyl Silyl Ethers **22** and **23** for 10 mM Solutions in CDCl_3 and $\text{CDCl}_3/\text{CD}_3\text{OD}$ Mixtures at 23° (in square brackets, $\Delta\delta$ values relative to CDCl_3 solution)

Ratio $\text{CDCl}_3/\text{CD}_3\text{OD}$	22			23	
	100:0 ^a)	100:3	10:1 ^a)	100:0	10:1
H–C(2/I) or H–C(5/I)	8.02	8.165	8.17 [0.15]	5.84	5.72 [–0.12]
H–C(8/I) or H–C(6/I)	8.135	8.09	8.03 [–0.105]	7.34	7.31 [–0.03]
H–C(1'/I)	6.185	6.17	6.14 [–0.045]	5.49	5.540 [0.05]
H–C(2'/I)	6.20 (br.)	5.90 (br.)	5.625 [–0.575]	5.26	5.022 [–0.24]
H–C(3'/I)	5.14	5.22	5.22 [0.08]	4.98	4.90 [–0.08]
H–C(4'/I)	4.58	4.475	4.385 [–0.195]	4.32	4.16 [–0.16]
H–C(5'/I)	4.98	4.945	4.95 [–0.03]	5.07	4.958 [–0.11]
H–C(2/II)	7.90	8.065	8.11 [0.21]	5.86	5.84 [–0.02]
H–C(1'/II)	6.045 (br.)	6.24	6.29 [0.245]	6.34	6.21 [–0.13]
H–C(2'/II) or H–C(5/II)	5.545	5.555	5.53 [–0.015]	5.31	5.20 [–0.11]
H–C(3'/II)	5.23	5.245	5.24 [0.01]	5.00	4.99 [–0.01]
H–C(4'/II)	4.235	4.27	4.24 [0.005]	4.12	4.08 [–0.04]
H–C(5'/II)	5.00	5.165	5.145 [0.145]	5.09	5.00 [–0.09]
H–C(5/III) or H–C(2/III)	coalescence	6.1–5.7	6.08 (br.)	7.98 (br.)	8.11 [0.13]
H–C(1'/III)	6.125	6.07	6.02 [–0.105]	6.16	6.18 [0.02]
H–C(2'/III)	5.32	5.143	5.07 [–0.25]	5.638	5.526 [–0.11]
H–C(3'/III)	4.91	4.93	4.92 [0.01]	5.39	5.36 [–0.03]
H–C(4'/III)	4.045	4.02	3.98 [–0.065]	4.29	4.23 [–0.06]
H–C(5'/III)	4.89	4.92	4.90 [0.01]	4.88	4.952 [0.07]
H–C(5/IV) or H–C(2/IV)	5.765	5.965	6.01 [0.245]	8.29	8.14 [–0.15]
H–C(1'/IV)	6.16	6.15	6.12 [–0.04]	6.10	6.07 [–0.03]
H–C(2'/IV)	5.32	5.185	5.11 [–0.21]	5.624	5.526 [–0.10]
H–C(3'/IV)	4.82	4.80	4.765 [–0.055]	5.13	5.04 [–0.09]
H–C(4'/IV)	4.095	4.075	4.04 [–0.055]	4.19	4.11 [–0.08]
H _a –C(5'/IV)	3.77	3.79	3.77 [0]	3.69	3.64 [–0.05]
H _b –C(5'/IV)	3.77	3.79	3.77 [0]	3.58	3.53 [–0.05]
$J(5,6\text{I})$	–	–	–	8.1	8.0
$J(1',2'\text{I})$	0	1.2	1.8	1.0	1.5
$J(2',3'\text{I})$	6.3	6.1	6.3	6.5	6.3
$J(3',4'\text{I})$	2.5	1.9	2.5	2.9	3.4
$J(4',5'\text{I})$	2.9	6.6	7.1	6.3	6.3
$J(1',2'\text{II})$	< 1.0	< 1.0	1.9	1.0	1.6
$J(2',3'\text{II})$	5.6	6.3	6.3	6.5	6.5
$J(3',4'\text{II})$	6.0	3.9	3.2	3.4	3.3
$J(4',5'\text{II})$	2.9	6.0	7.6	6.3	7.8
$J(1',2'\text{III})$	< 1.0	< 1.0	0.9	0	1.3
$J(2',3'\text{III})$	6.1	6.0	6.2	6.2	6.2
$J(3',4'\text{III})$	3.0	4.9	5.1	5.0	3.6
$J(4',5'\text{III})$	6.3	5.9	6.3	7.0	7.7
$J(1',2'\text{IV})$	1.1	0.9	0.9	1.4	1.9
$J(2',3'\text{IV})$	6.6	6.3	6.3	6.2	6.2
$J(3',4'\text{IV})$	4.1	4.3	4.5	3.9	3.4
$J(4',5'_a\text{IV})$	6.3	6.6	6.3	6.8	7.0
$J(4',5'_b\text{IV})$	6.3	6.6	6.3	6.8	6.2
$J(5'_a,5'_b\text{IV})$	b)	b)	b)	10.4	10.5

^a) Assignments based on DQF-COSY, HSQC, and HMBC spectra. ^b) Not determined.

of the signals of **22** in both solvents is based on DQFCOSY, HSQC, and HMBC spectra.

The $J(4',5'/I_A)$ and $J(4',5'/II_A)$ values of **22** are small in $CDCl_3$ (2.9 Hz), and increase to 7.1–7.6 Hz in $CDCl_3/CD_3OD$ 10:1. These values evidence a mixture of cyclic duplexes (*gauche*-oriented H-atoms) and of the simplex (preferred antiperiplanar H-atoms). The value of $J(4',5'/III_U) = 5.9$ –6.3 Hz does not depend upon the solvent, in agreement with the finding that the ethynyl group in cyclic $A^*[c_v]U^{(*)}$ duplexes adopts a non-staggered orientation between *gg* and a synperiplanar orientation to C(3') [1]. The $J(4',5'/III_A)$ value of **23** is large in both solvents (7.0 Hz in $CDCl_3$ and 7.7 Hz in $CDCl_3/CD_3OD$ 10:1), and shows a weak solvent dependence (6.3 vs. 7.8 Hz), similarly as $J(4',5'/II_U)$, whereas $J(4',5'/I_U) = 6.3$ Hz does not depend upon the solvent. This evidences an orientation of unit IV of **23** that is hardly compatible with its involvement in a cyclic duplex.

Upon addition of 10% of CD_3OD , H–C(2'/I_A) of **22** is shifted upfield from 6.20 to 5.625 ppm. Similarly, H–C(2'/I_U) of **23** is shifted from 5.26 to 5.02 ppm (Table 2). H–C(2'/II_A) of a solution of **22** in $CDCl_3/CD_3OD$ 10:1 resonates at 5.53 ppm and H–C(2'/II_U) of **23** at 5.20 ppm. This evidences that the large upfield shift for H–C(2'/I_A) of **22** ($\Delta\delta = 0.575$ ppm) is due to dissociation of the duplexes, whereas the smaller upfield shift for H–C(2'/I_A) of **23** in $CDCl_3/CD_3OD$ 10:1 ($\Delta\delta = 0.24$ ppm) is also due to a stronger preference for the *anti*-conformation. Apart from H–C(2'/I_A), the CH signals of **22** ($\Delta\delta \leq 0.25$ ppm) show a stronger solvent dependence than those of **23** ($\Delta\delta \leq 0.16$ ppm), confirming the stronger tendency of **22** to form cyclic duplexes. The HN(3) and H₂N–C(6) signals of **22** in $CDCl_3$ are hidden, due to coalescence, whereas HN(3/I–II) of **23** resonates at 11.6 ppm, and H₂N–C(6/III–IV) at 6.35 and 6.45 ppm. The weak downfield shifts for **23**, as compared to the $\delta(HN(3))$ and $\delta(H_2N-C(6))$ values of *Watson–Crick* base-paired cyclic duplexes derived from the corresponding dimers (12.3–13.4 and 6.7–7.0 ppm [1]), suggest the predominant formation of linear duplexes. In view of these results, we investigated the duplex formation of **22** in more depth.

To analyse the solvent dependence of the association of **22** in more detail, we recorded ¹H-NMR spectra of 10 mM solutions in $CDCl_3/CD_3OD$ 100:0 to 100:10, starting with a solution in $CDCl_3$ and repetitively adding 1% of CD_3OD . A simplex/duplexes equilibrium in $CDCl_3$ is evidenced by the absence of the HN(3), H₂N–C(6), and H–C(5/III) signals, due to coalescence. The signal of H–C(5/III) appeared in $CDCl_3/CD_3OD$ 100:3. Although it was sharpened by adding further amounts of CD_3OD , it remained significantly broader than the H–C(5/IV) *s*, even in $CDCl_3/CD_3OD$ 10:1. Other signals, especially those of H–C(2'/I) and H–C(1'/II), are broad in $CDCl_3$ and better resolved upon the addition of CD_3OD . Chemical-shift differences of signals showing maximal shift differences above 0.03 ppm relative to the spectrum of the solution in $CDCl_3$ are depicted in Fig. 4. A dependence of the chemical shift on the CD_3OD content of $CDCl_3$ is only detectable up to a concentration of 8% CD_3OD , evidencing that the transformation into a solvated simplex is completed. The largest upfield shifts are observed for H–C(2'/I), H–C(2'/III), H–C(2'/IV), and H–C(4'/I) (–0.575, –0.25, –0.21, and –0.195 ppm, resp.), whereas H–C(2'/II) shows only a weak upfield shift of 0.015 ppm. The largest downfield shifts are observed for H–C(5/IV), H–C(2/II), H–C(2/I), H–C(1'/II), and H–C(5'/II) (0.245, 0.21, 0.15, 0.245, and

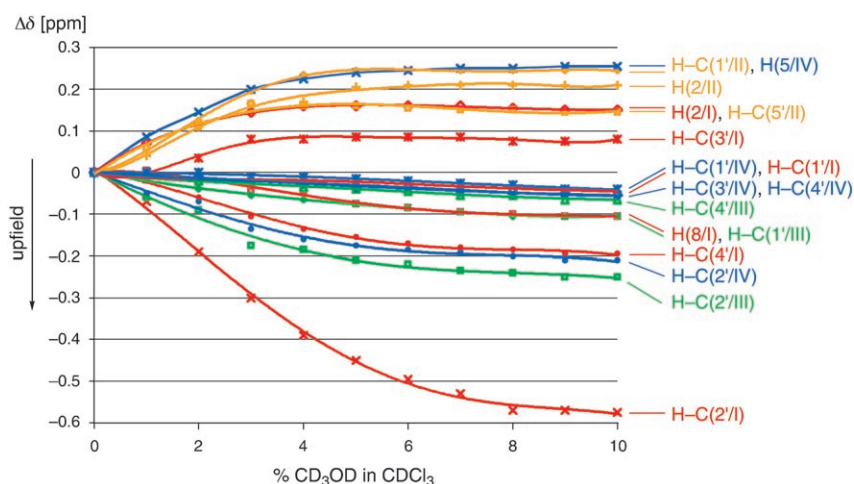


Fig. 4. Chemical-shift differences [ppm] for selected CH signals of **22** in $CDCl_3/CD_3OD$ 100:1 to 100:10 relative to the spectrum in pure $CDCl_3$ (trend lines obtained by the programme Microsoft Excel)

0.145 ppm, resp.). The upfield shifts for H–C(2') and the downfield shift of the CH signals of the nucleobases are in agreement with the observation that the formation of cyclic duplexes of the self-complementary $U^*[c_y]A^{(*)}$ and $A^*[c_y]U^{(*)}$ dimers leads to a downfield shift of H–C(2') and to an upfield shift of the CH of the nucleobases [1].

The coalescence of the NH signals of **22** in $CDCl_3$ at ambient temperature prevents the determination of the concentration dependence of its chemical shift and the calculation of the thermodynamic parameters by *van't Hoff* analysis.

To gain more information about duplex formation, we determined the temperature dependence of the 1H -NMR chemical shifts of a 10 mM solution of **22** in $CDCl_3$ between 223 and 323 K in 10 K steps. However, in the absence of sufficient information about the structure of the associates, it proved difficult to rationalise the size and the sign of the shifts described below.

The chemical shifts of the CH signals at temperatures between 223 and 323 K in 20 K steps are given in Table 3, and the temperature effect on the chemical shift is depicted in Fig. 5 (only for signals showing a maximal shift difference above 0.07 ppm). Two CH signals show coalescence, H–C(5/III_U) at 293–323 K and H–C(2'/I_A) at 253–263 K. At 223 and 233 K, all signals are broad due to the high viscosity of the solvent. Largest shift differences are observed for CH groups of units I and II. With increasing temperature, the unit II H–C(2), H–C(2'), H–C(1'), H–C(5'), and H–C(4') signals are shifted downfield ($\Delta\delta_{\max} = 0.33, 0.32, 0.21, 0.19,$ and 0.12 ppm, resp.). The unit I H–C(2'), H–C(4'), and H–C(8) signals are shifted upfield ($\Delta\delta_{\max} = -0.24, -0.08,$ and -0.08 ppm, resp.), while those of H–C(2) and H–C(3') are shifted downfield ($\Delta\delta_{\max} = 0.315$ and 0.085 ppm, resp.). The strong upfield shift for H–C(2'/I) reflects decreasing amounts of cyclic duplexes with increasing temperature; the temperature and the above discussed solvent effects run parallel.

Considering the difficult interpretation of these observations, we attempted to analyse the duplex formation on the basis of the temperature dependence of the HN(3)

Table 3. Temperature Dependence of Selected $^1\text{H-NMR}$ Chemical Shifts [ppm] of the Tetrameric Tripropargyl Silyl Ether **22** for 10 mM Solution in CDCl_3 (in square brackets, $\Delta\delta$ values relative to the solution at 223 K)

Temperature [K]	223	243	263	283	303	323
H–C(2/I)	7.80	7.855	7.915	7.985	8.045	8.115 [0.315]
H–C(8/I)	8.17	8.18	8.165	8.155	8.12	8.09 [–0.08]
H–C(1'/I)	6.19	6.19	6.19	6.185	6.185	6.185 [–0.005]
H–C(2'/I)	6.40	6.35 (br.)	6.3–6.1	6.18 (br.)	6.165	6.16 [–0.24]
H–C(3'/I)	5.11	5.11	5.115	5.125	5.155	5.195 [0.085]
H–C(4'/I)	4.61	4.62	4.61	4.60	4.57	4.53 [–0.08]
H–C(5'/I)	4.94	4.95	4.995	4.97	4.985	4.995 [0.055]
H–C(2/II)	7.70	7.745	7.775	7.85	7.935	8.03 [0.33]
H–C(1'/II)	5.92	5.925	5.945 (br.)	6.00 (br.)	6.07 (br.)	6.13 [0.21]
H–C(2'/II)	5.32	5.325	5.41	5.495	5.575	5.64 [0.32]
H–C(3'/II)	5.21	5.21	5.21	5.225	5.235	5.25 [0.04]
H–C(4'/II)	4.15	4.175	4.195	4.215	4.24	4.27 [0.12]
H–C(5'/II)	4.89	4.90	4.95	4.97	5.02 (br.)	5.08 [0.19]
H–C(5/III)	5.99	6.00	6.3–5.9	6.2–5.9	coalescence	coalescence
H–C(1'/III)	6.115	6.115	6.115	6.12	6.128	6.13 [0.015]
H–C(2'/III)	5.32	5.325	5.33	5.325	5.32	5.305 [–0.015]
H–C(3'/III)	4.81	4.82	4.84	4.90	4.91	4.95 [0.14]
H–C(4'/III)	3.98	4.005	4.015	4.03	4.05	4.07 [0.09]
H–C(5'/III)	4.81	4.82	4.84	4.88	4.905	4.94 [0.13]
H–C(5/IV)	5.75	5.74	5.74	5.76	5.775	5.80 [0.05]
H–C(1'/IV)	6.14	6.14	6.15	6.157	6.165	6.165 [0.025]
H–C(2'/IV)	5.32	5.325	5.33	5.325	5.32	5.305 [–0.015]
H–C(3'/IV)	4.79	4.80	4.805	4.81	4.82	4.835 [0.045]
H–C(4'/IV)	4.11	4.095	4.095	4.095	4.095	4.095 [–0.015]
2 H–C(5'/IV)	3.72	3.73	3.745	3.76	3.775	3.795 [0.075]

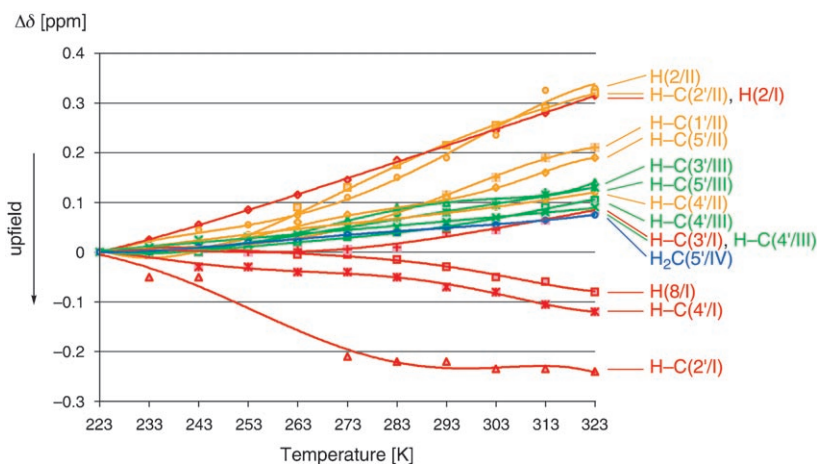


Fig. 5. Chemical-shift differences [ppm] for selected CH signals for a 10 mM Solution of **22** at 223 to 323 K in CDCl_3 (in 10 K steps) relative to the spectrum at 223 K (trend lines obtained by the programme Microsoft Excel)

signals of **22** in CDCl_3 in the temperature range of 323 to 223 K. The HN(3/III–IV) signals of **22** are hidden in the CDCl_3 spectra recorded at 323–293 K. A broad *s* appearing at 13.8 ppm at 283 K became increasingly sharper as the temperature was lowered to 253 K. Two uridine NH signals of equal intensity, a broad *s* at 13.75 and a twice as broad *s* at 14.3 ppm, are visible at a temperature of 243 K. At 233 K, there are three uridine NH *ss* (at 14.6, 14.35, and 13.73 ppm) with an intensity ratio of 1:2.2. Lowering the temperature to 223 K had little effect on the chemical shift of these signals, appearing at 14.65, 14.45, and 13.73 ppm, but the intensity changed to 2:1:1. This evidences a contribution of two or several cyclic duplexes, connected by *Watson–Crick*- (HN(3) at 14.6 and 14.4 ppm) and/or *Hoogsteen*-type base pairing (HN(3) at 13.7 ppm⁴). In parallel with the uridine HN(3) signal, a broad *s* for the adenine $\text{H}_2\text{N}-\text{C}(6)$ at 8.6 ppm at 283 K was narrowed upon cooling to 243 K. At 233 and 223 K, this signal split into several broad *ss*. Their overlap with the broad signals of H–C(2/I), H–C(8/I), and H–C(2/II) prevents an unambiguous assignment.

To gain information about base stacking, we measured the CD spectra of 0.2 mM solutions of **22** in CHCl_3 and $\text{CHCl}_3/\text{MeOH}$ 10:1 in the temperature range from -10 to 50° in 10° steps (Fig. 6). The weak temperature-dependence evidences the absence of base stacking and of significant amounts of cyclic duplexes under the selected experimental conditions of concentration, solvent, and temperature. No duplex was expected for solutions in $\text{CHCl}_3/\text{MeOH}$ 10:1, as discussed above, and a low simplex/cyclic duplex equilibrium constant must be responsible for the absence of cyclic duplexes in a 0.2 mM solution of **22** in CHCl_3 .

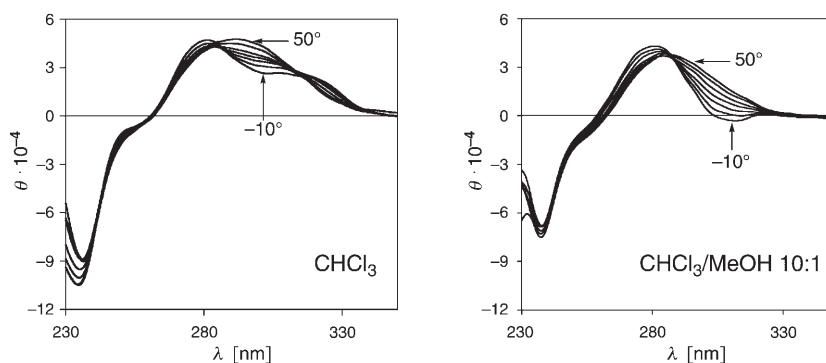


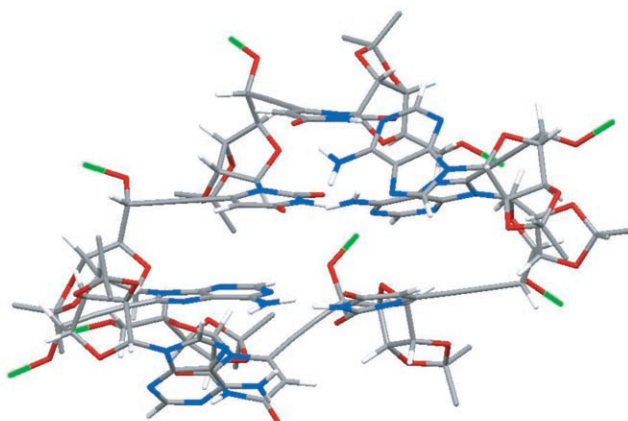
Fig. 6. CD spectra of 0.2 mM solutions of **22** in CHCl_3 and in $\text{CHCl}_3/\text{MeOH}$ 10:1 recorded at -10 to 50° in 10° steps

Unfortunately, our NMR equipment did not allow measuring low-temperature ROESY spectra that would supply spectroscopic evidence for the type of base pairing involved in duplex formation.

⁴) The chemical shift values for HN(3) of uridine units involved in *Watson–Crick*- or *Hoogsteen*-type base pairing differ by 0.8–1.0 ppm [1][14]. A comparison with the typical shift values at room temperature (12.3–12.8 and 11.5–11.9 ppm) evidences a downfield shift of 2 ppm for both base-pairing types upon lowering the temperature.

Maruzen modeling showed that **22** can form cyclic duplexes connected by either *Watson–Crick*- or *Hoogsteen*-type H-bonds, but not by both of them, since the distance between the nucleobases is larger by 2 Å in a *Watson–Crick*-type than in a *Hoogsteen*-type base pair ($C(1'/A) \cdots C(1'/U)$ distances are *ca.* 10.8 and 8.8 Å, resp.). A right-handed duplex of **22** possessing four *Watson–Crick* base pairs was modeled with the *Amber** force field [15]. Constraints were first set to generate a structure agreeing with the NMR data, and then released. The optimized duplex retained the *Watson–Crick* base pairing (Fig. 7). The calculated $J(4',5')$ values of the $A^{(*)}$ units I and II (4.1, 1.0, 2.1, and 5.1 Hz) agree fairly well with the experimental $J(4',5')$ value of 2.9 Hz, whereas the

Front view:



Top view

(from top to bottom, the H-bonds are marked with bold, solid, hashed, and dashed lines, resp.):

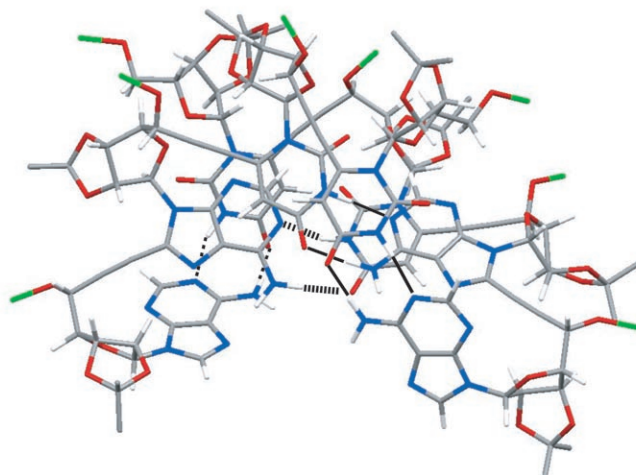


Fig. 7. Front and top view of an *AMBER**-modeled right-handed duplex of **22** connected by *Watson–Crick* base pairing (substituents at Si- and H-atoms of isopropylidene groups omitted for enhanced clarity)

calculated $J(4',5')$ values of the U* units III (3.7 and 4.7 Hz) are smaller than the experimental $J(4',5')$ value of 6.3 Hz. The central units show moderate and the terminal units large propeller (-18 and -24° vs. $+40^\circ$) and buckle twists (22 and 28° vs. 48 and 73°). This suggests some ring strain upon forming cyclic duplexes connected by four base pairs, in agreement with the observation of an equilibrium between simplex and several duplexes. The duplex depicted in Fig. 4 may not be the most stable one; on account of insufficient spectroscopic data we did not perform further *Amber** calculations.

Modeling the duplex of **22** suggested that the bulky $(\text{Me}_2\text{CH})_3\text{SiO}$ groups destabilise the cyclic duplexes, and that further studies of self-complementary tetramers should be conducted with deoxygenated analogues.

We thank the *ETH Zürich* and *F. Hoffmann-La Roche AG*, Basel, for generous support, Mrs. *B. Brandenberg* for recording the 2D-NMR spectra, and Prof. *B. Jaun* for helpful discussions.

Experimental Part

General. See [4]. For the NMR titration and *van't Hoff* analysis, see [1]. For selected $^1\text{H-NMR}$ data of the monomers **3**, **9**, **11**, and **15**, see Table 4.

9-(6,7-Dideoxy-2,3-O-isopropylidene- β -D-allo-hept-6-ynofuranosyl)adenin-8-yl-(8 \rightarrow 7'-C)-9-(6,7-dideoxy-2,3-O-isopropylidene- β -D-allo-hept-6-ynofuranosyl)adenine (5). A soln. of **4** [2] (100 mg, 0.14 mmol) in THF (10 ml) was treated with $\text{Bu}_4\text{NF} \cdot 3 \text{H}_2\text{O}$ (54 mg, 0.16 mmol), stirred for 2 h at 25° , and evaporated. FC ($\text{CHCl}_3/\text{MeOH}$ 15:1) gave **5** (86 mg, 93%). White solid. R_f ($\text{CHCl}_3/\text{MeOH}$ 15:1)

Table 4. Selected $^1\text{H-NMR}$ Chemical Shifts [ppm] and Coupling Constants [Hz] of the Uridine Monomers **3** and **9**, and the Adenosine Monomers **11** and **15**^{a)}

	3	9 (2 mM)	9 (4 mM)	9	11	15 (2 mM)	15 (4 mM)	15
$\text{CDCl}_3/(\text{D}_6)\text{DMSO}$	0:1	1:0	10:1	0:1	0:1	1:0	10:1	0:1
H–C(5) or H–C(2)	6.36	5.74	5.43	5.62	8.06	8.30	8.06	8.14
H–C(6) or H–C(8)	–	7.40	7.49	7.75	–	7.84	7.77	8.30
HN(3) or H_2N –C(6)	11.67	7.98	10.64	11.41	7.56	5.61	6.21	7.36
H–C(1')	6.00	5.63	5.73	5.85	5.96	5.85	5.77	6.15
H–C(2')	5.21	5.00	4.57	4.90	5.66	5.14	4.95	5.30
H–C(3')	4.84	5.07	4.80	4.86	5.09	5.22	4.99	5.06
H–C(4')	3.83	4.35	4.09	4.02	4.05	4.57	4.33	4.17
H–C(5')	4.25	4.67	4.35	4.40	4.29	4.74	4.49	4.40
HO–C(5')	5.87	3.23	5.53	6.08	6.30	7.76	7.41	6.29
H–C(7')	–	2.60	2.42	3.42	–	2.57	2.44	3.19
$J(5,6)$	–	8.1	7.8	8.1	–	–	–	–
$^4J(5,\text{NH})$	2.1	0	0	0	–	–	–	–
$J(1',2')$	0.9	3.6	3.6	2.4	2.7	5.1	4.8	3.3
$J(2',3')$	6.6	6.2	6.3	6.3	6.0	6.0	6.3	6.3
$J(3',4')$	3.3	2.4	2.7	2.4	2.1	0.6	0.9	2.1
$J(4',5')$	9.0	2.7	3.3	5.4	7.5	2.1	2.1	5.1
$J(5',\text{OH})$	^{b)}	3.0	4.5	5.7	5.1	1.8	2.4	5.1
$J(5',7')$	–	2.4	2.1	2.1	–	2.4	2.1	2.1

^{a)} Assignments based on selective homodecoupling experiments. ^{b)} Not assigned (broad H–C(5') and HO–C(5') signal).

0.17. M.p. 182–184°. $[\alpha]_D^{25} = -101.2$ ($c = 0.5$, CHCl_3). UV (CHCl_3): 267 (22000), 295 (21000). IR (ATR): 3441w, 3179w, 2988w, 2864w, 2240w, 1638s, 1597m, 1577m, 1477w, 1375m, 1329w, 1270w, 1213m, 1155w, 1076s, 969w, 852m, 797m, 751w, 647m. $^1\text{H-NMR}$ (300 MHz, (D_6) DMSO): see Table 5; additionally, 1.56, 1.50, 1.35, 1.30 (4s, 2 Me_2C). $^{13}\text{C-NMR}$ (75 MHz, (D_6) DMSO): see Table 6; additionally, 113.34 (s, 2 Me_2C); 26.98, 25.18 (2q, 2 Me_2C). HR-MALDI-MS: 683.2313 ($[M + \text{Na}]^+$, $\text{C}_{30}\text{H}_{32}\text{N}_{10}\text{NaO}_8^+$; calc. 683.2302).

1-(6,7-Dideoxy-2,3-O-isopropylidene- β -D-allo-hept-6-ynofuranosyl)uracil-6-yl-(6 \rightarrow 7'-C)-9-(6,7-dideoxy-2,3-O-isopropylidene- β -D-allo-hept-6-ynofuranosyl)adenin-8-yl-(8 \rightarrow 7'-C)-9-(6,7-dideoxy-2,3-O-isopropylidene- β -D-allo-hept-6-ynofuranosyl)adenine (**6**). A soln. of **3** [**5**] (60 mg, 0.11 mmol), **5** (58 mg, 0.09 mmol), $[\text{Pd}_2(\text{dba})_3]$ (8 mg, 0.009 mmol), CuI (3.5 mg, 0.017 mmol), and $\text{P}(\text{fur})_3$ (3.3 mg, 0.014 mmol) in degassed Et_3N /toluene 1:1 (7 ml) was stirred for 16 h at 25°. Evaporation and FC ($\text{CHCl}_3/\text{MeOH}$ 16:1) gave the C-silylated trimer (62 mg, R_f ($\text{CHCl}_3/\text{MeOH}$ 15:1) 0.25), which was dissolved in THF (9 ml), treated dropwise with a soln. of $\text{Bu}_4\text{NF} \cdot 3 \text{H}_2\text{O}$ (27 mg, 0.086 mmol) in THF

Table 5. Selected $^1\text{H-NMR}$ Chemical Shifts [ppm] and Coupling Constants [Hz] of the Dimers **5**, **10**, **16**, and **19** in (D_6) DMSO

Sequence	5 AA	10 UU	16 UA	19 AU
H–C(5/I) or H–C(2/I)	8.15	5.62	8.15	5.64
H–C(6/I) or H–C(8/I)	8.32	7.72	8.30	7.76
HN(3/I) or H_2N –C(6/I)	7.38	11.43	7.36	11.45
H–C(1'/I)	6.24	5.84	6.21	5.87
H–C(2'/I)	5.39	5.00	5.39	5.02
H–C(3'/I)	5.19	4.90	5.13	4.95
H–C(4'/I)	4.29	4.08	4.24	4.14
H–C(5'/I)	4.83	4.75	4.78	4.79
HO–C(5'/I)	6.67	6.53	6.68	6.54
H–C(5/II) or H–C(2/II)	8.16	5.89	5.83	8.17
HN(3/II) or H_2N –C(6/II)	7.67	11.68	11.67	7.68
H–C(1'/II)	6.10	6.08	6.04	6.14
H–C(2'/II)	5.40	5.20	5.17	5.44
H–C(3'/II)	5.10	4.85	4.83	5.11
H–C(4'/II)	4.10	3.83	3.83	4.09
H–C(5'/II)	4.42	4.27	4.25	4.43
HO–C(5'/II)	6.36	5.83	5.82	6.35
H–C(7'/II)	3.27	3.22	3.21	3.27
$J(5,6/I)$	–	8.1	–	8.1
$^4J(5,\text{NH}/I)$	–	2.1	–	2.1
$J(1',2'/I)$	2.7	2.1	2.7	2.4
$J(2',3'/I)$	6.3	6.6	6.3	6.3
$J(3',4'/I)$	2.4	3.3	2.4	3.3
$J(4',5'/I)$	6.6	6.6	6.3	6.6
$J(5',\text{OH}/I)$	5.7	6.3	6.0	6.0
$^4J(5,\text{NH}/II)$	–	1.2	0	–
$J(1',2'/II)$	3.3	1.8	1.5	3.0
$J(2',3'/II)$	6.6	6.6	6.3	6.3
$J(3',4'/II)$	2.4	3.3	3.3	2.4
$J(4',5'/II)$	6.6	9.0	9.0	6.9
$J(5',\text{OH}/II)$	5.1	6.6	6.6	5.7
$J(5',7'/II)$	1.8	2.1	2.1	2.1

Table 6. Selected ^{13}C -NMR Chemical Shifts [ppm] of the Dimers **5**, **10**, **16**, and **19** in (D_6)DMSO

Sequence	5	10	16	19	5	10	16	19
	AA	UU	UA	AU	AA	UU	UA	AU
C(2/I)	152.71	150.35	152.50	150.38	C(2/II)	153.70	149.84	149.60
C(4/I)	148.64	163.20	148.43	163.22	C(4/II)	147.90	161.88	161.60
C(5/I)	119.02	101.75	118.88	101.88	C(5/II)	118.94	108.10	107.98
C(6/I)	156.18 ^{a)}	142.54	155.96	142.58	C(6/II)	156.12 ^{a)}	136.01	135.76
C(8/I)	139.86	–	139.69	–	C(8/II)	132.09	–	132.20
C(1'/I)	89.79	92.40	90.25	92.36	C(1'/II)	90.40	93.74	93.66
C(2'/I)	83.30	83.36 ^{a)}	83.18	83.46	C(2'/II)	81.96	83.52 ^{a)}	83.18
C(3'/I)	81.39	80.93	81.24	80.93	C(3'/II)	81.39	82.44	82.30
C(4'/I)	87.87	88.00	87.58	88.07	C(4'/II)	88.06	90.43	89.58
C(5'/I)	61.76	61.62	61.78	61.53	C(5'/II)	61.26	61.12	61.06
C(6'/I)	95.28	101.85	101.30	95.41	C(6'/II)	83.09	84.68	84.54
C(7'/I)	73.40	75.22 ^{b)}	75.01	73.37	C(7'/II)	75.99	75.27 ^{b)}	75.24

^{a)} ^{b)} Assignments may be interchanged.

(2 ml), and stirred for 2 h at 25°. Evaporation and FC ($\text{CHCl}_3/\text{MeOH}$ 10:1) gave **6** (38 mg, 45%). Pale yellow solid. R_f ($\text{CHCl}_3/\text{MeOH}$ 15:1) 0.19. M.p. 214° (dec.). $[\alpha]_{\text{D}}^{25} = -60.2$ ($c = 1.0$, CHCl_3). UV (CHCl_3): 294 (32200). IR (ATR): 3333w, 3180w, 2988w, 2240w, 1694m, 1637s, 1596m, 1375m, 1329m, 1300w, 1269w, 1214s, 1155w, 1076s, 853m, 797w, 760w, 648w. $^1\text{H-NMR}$ (500 MHz, (D_6)DMSO): see Table 7; additionally, 1.56, 1.53, 1.37, 1.35, 1.32, 1.22 (6s, 3 Me_2C). $^{13}\text{C-NMR}$ (125 MHz, (D_6)DMSO): see Table 8; additionally, 113.33, 113.49, 112.49 (3s, 3 Me_2C); 27.00, 26.95, 26.70, 25.21, 25.20, 25.12 (6q, 3 Me_2C). HR-MALDI-MS: 989.3195 ($[M + \text{Na}]^+$, $\text{C}_{44}\text{H}_{46}\text{N}_{12}\text{NaO}_{14}$; calc. 989.3154).

2',3'-O-Isopropylidene-5'-O-(triisopropylsilyl)uridin-6-yl-(6 → 7'-C)-1-(6,7-dideoxy-2,3-O-isopropylidene-β-D-allo-hept-6-ynofuranosyl)uracil-6-yl-(6 → 7'-C)-9-(6,7-dideoxy-2,3-O-isopropylidene-β-D-allo-hept-6-ynofuranosyl)adenin-8-yl-(8 → 7'-C)-9-(6,7-dideoxy-2,3-O-isopropylidene-β-D-allo-hept-6-ynofuranosyl)adenine (**8**). A soln. of **7** [5] (59.5 mg, 0.11 mmol), **6** (67.6 mg, 0.07 mmol), $[\text{Pd}_2(\text{dba})_3]$ (6.2 mg, 0.007 mmol), CuI (2.9 mg, 0.014 mmol), and P(fur)₃ (3.0 mg, 0.011 mmol) in degassed $\text{Et}_3\text{N}/\text{toluene}$ 1:1 (6 ml) was stirred for 16 h at 25°. Evaporation and FC ($\text{CHCl}_3/\text{MeOH}$ 15:1) gave **8** (32 mg, 34%). Pale yellow solid. R_f ($\text{CHCl}_3/\text{MeOH}$ 10:1) 0.34. M.p. 218° (dec.). $[\alpha]_{\text{D}}^{25} = -15.2$ ($c = 1.0$, CHCl_3). UV (CHCl_3): 285 (22600). IR (ATR): 3320w, 3188w, 2926m, 2864w, 2240w, 1693s, 1639s, 1597m, 1455w, 1374s, 1329w, 1300w, 1261w, 1211m, 1156m, 1067s, 866m, 797m, 762w, 682w, 647w. $^1\text{H-NMR}$ (500 MHz, (D_6)DMSO): see Table 9; additionally, 1.56, 1.52, 1.40, 1.39, 1.35, 1.31, 1.24, 1.23 (8s, 4 Me_2C); 1.06–0.98 (m, (Me_2CH)₃Si). $^{13}\text{C-NMR}$ (125 MHz, (D_6)DMSO): see Table 10; additionally, 113.44, 113.28, 112.72, 112.50 (4s, 4 Me_2C); 26.94, 26.92, 26.84, 26.67, 25.22, 25.18, 25.17, 25.07 (8q, 4 Me_2C); 17.72, 17.67 (2q, (Me_2CH)₃Si); 11.32 (d, (Me_2CH)₃Si). HR-MALDI-MS: 1427.528 ($[M + \text{Na}]^+$, $\text{C}_{65}\text{H}_{80}\text{N}_{14}\text{NaO}_{20}\text{Si}$; calc. 1427.534). Anal. calc. for $\text{C}_{65}\text{H}_{80}\text{N}_{14}\text{O}_{20}\text{Si}$ (1405.51): C 55.55, H 5.74, N 13.95; found: C 55.30, H 5.76, N 13.73.

1-(6,7-Dideoxy-2,3-O-isopropylidene-β-D-allo-hept-6-ynofuranosyl)uracil-6-yl-(6 → 7'-C)-1-(6,7-dideoxy-2,3-O-isopropylidene-β-D-allo-hept-6-ynofuranosyl)uracil (**10**). A soln. of **3** (492 mg, 0.9 mmol), **9** [5] (241 mg, 0.78 mmol), $[\text{Pd}_2(\text{dba})_3]$ (34.8 mg, 0.039 mmol), CuI (16.7 mg, 0.078 mmol), and P(fur)₃ (16.6 mg, 0.062 mmol) in degassed $\text{Et}_3\text{N}/\text{toluene}$ 1:1 (16 ml) was stirred for 18 h at 25°. Evaporation and FC ($\text{CHCl}_3/\text{MeOH}$ 30:1) gave the C-silylated dimer (513 mg; R_f ($\text{CHCl}_3/\text{MeOH}$ 15:1) 0.30), which was dissolved in THF (10 ml), treated dropwise with a soln. of $\text{Bu}_4\text{NF} \cdot 3 \text{H}_2\text{O}$ (333 mg, 1.06 mmol) in THF (5 ml), and stirred for 2 h at 24°. Evaporation and FC ($\text{CHCl}_3/\text{MeOH}$ 20:1) gave **10** (302 mg, 63%). Pale yellow solid. R_f ($\text{CHCl}_3/\text{MeOH}$ 10:1) 0.36. M.p. 221–222°. $[\alpha]_{\text{D}}^{25} = +10.8$ ($c = 1.0$, CHCl_3). UV (CHCl_3): 262 (7700). IR (ATR): 3251w, 2987w, 2800w, 2257w, 1682s, 1597w, 1455m, 1378m, 1268m, 1210m, 1157w, 1058s, 1023s, 1000s, 865m, 821m, 761m, 715w, 664w, 628w. $^1\text{H-NMR}$ (300 MHz, (D_6)DMSO): see Table 5; additionally, 1.48, 1.43, 1.30, 1.26 (4s, 2 Me_2C). $^{13}\text{C-NMR}$ (75 MHz, (D_6)DMSO): see Table 6;

Table 7. Selected $^1\text{H-NMR}$ Chemical Shifts [ppm] and Coupling Constants [Hz] of the Trimers **6**, **12**, **17**, and **20** in (D_6)DMSO^a

Sequence	6					6			
	UAA	AUU	AUA	UAU		UAA	AUU	AUA	UAU
H–C(5/I) or H–C(2/I)	8.16	5.63	8.16	5.64					
H–C(6/I) or HC(8/I)	8.33	7.72	8.30	7.77	$J(5,6/I)$	–	7.9	–	8.0
HN(3/I) or H ₂ N–C(6/I)	7.37	11.42	7.34	11.44					
H–C(1'/I)	6.24	5.84	6.22	5.88					
H–C(2'/I)	5.41	5.01	5.38	5.02	$J(1',2'/I)$	3.0	2.2	2.7	2.6
H–C(3'/I)	5.20	4.92	5.15	4.96	$J(2',3'/I)$	6.4	6.4	6.2	6.4
H–C(4'/I)	4.31	4.10	4.27	4.16	$J(3',4'/I)$	2.5	3.4	2.5	2.9
H–C(5'/I)	4.84	4.76	4.80	4.84–4.80	$J(4',5'/I)$	6.2	6.6	6.3	6.2
HO–C(5'/I)	6.69	6.52	6.68	6.54	$J(5',\text{OH}/I)$	5.6	5.9	5.9	5.9
H–C(5/II) or H–C(2/II)	8.18	5.91	5.84	8.19					
HN(3/II) or H ₂ N–C(6/II)	7.65	11.71	11.70	7.65					
H–C(1'/II)	6.18	6.16	6.12	6.21					
H–C(2'/II)	5.49	5.26	5.23	5.50	$J(1',2'/II)$	2.7	1.4	1.4	2.6
H–C(3'/II)	5.18	4.96	4.95	5.20	$J(2',3'/II)$	6.4	6.6	6.4	6.4
H–C(4'/II)	4.21	4.03	4.03	4.20	$J(3',4'/II)$	2.7	3.5	3.3	2.8
H–C(5'/II)	4.80	4.69	4.68	4.84–4.80	$J(4',5'/II)$	7.3	9.1	9.0	7.5
HO–C(5'/II)	6.72	6.38	6.36	6.71	$J(5',\text{OH}/II)$	5.9	6.8	6.9	6.0
H–C(5/III) or H–C(2/III)	5.88	8.17	8.17	5.82					
HN(3/III) or H ₂ N–C(6/III)	11.66	7.65	7.65	11.65					
H–C(1'/III)	6.00	6.13	6.12	6.00					
H–C(2'/III)	5.16	5.42	5.42	5.16	$J(1',2'/III)$	1.4	3.4	3.6	1.5
H–C(3'/III)	4.83	5.11	5.10	4.84–4.80	$J(2',3'/III)$	6.4	6.1	6.1	6.4
H–C(4'/III)	3.83	4.13	4.12	3.82	$J(3',4'/III)$	3.0	2.2	2.2	3.2
H–C(5'/III)	4.27	4.46	4.46	4.26	$J(4',5'/III)$	9.0	6.6	6.7	8.8
HO–C(5'/III)	5.81	6.40	6.39	5.81	$J(5',\text{OH}/III)$	6.4	4.9	5.3	6.3
H–C(7'/III)	3.20	3.25	3.25	3.19	$J(5',7'/III)$	2.1	2.2	2.1	1.9

^a) Assignments based on DQFCOSY, HSQC, and HMBC spectra.Table 8. Selected $^{13}\text{C-NMR}$ Chemical Shifts [ppm] of the Trimers **6**, **12**, **17**, and **20** in (D_6)DMSO^a

Sequence	6					6			
	UAA	AUU	AUA	UAU		UAA	AUU	AUA	UAU
C(2/I)	152.70	150.31	153.49	150.37	C(2/III)	149.81	153.56	152.59	149.80
C(4/I)	148.65	163.17	148.54	163.19	C(4/III)	161.91	147.86	147.78	161.83
C(5/I)	119.04	101.80	118.97	101.87	C(5/III)	108.17	118.98	118.90	108.10
C(6/I)	156.19 ^b	142.54	156.09 ^b	142.50	C(6/III)	135.60	156.10	156.01 ^b	135.97
C(8/I)	139.92	–	139.76	–	C(8/III)	–	132.41	132.32	–
C(1'/I)	89.90	92.45	89.61	92.39	C(1'/III)	95.30	90.48	90.41	93.56
C(2'/I)	83.29	83.49	82.98	83.52	C(2'/III)	82.30	81.94	81.85	82.41
C(3'/I)	81.66	80.89	81.17	80.93	C(3'/III)	82.38	81.44	81.36	82.37
C(4'/I)	87.86	88.01	87.55	88.05	C(4'/III)	90.02	88.04	87.93	90.30
C(5'/I)	61.80	61.65	61.78	61.56	C(5'/III)	61.09	61.34	61.25	61.08
C(6'/I)	95.30	101.82	101.48	95.49	C(6'/III)	84.62	83.05	83.33	84.61
C(7'/I)	73.52	75.02	74.95	73.50	C(7'/III)	74.81	75.86	75.79	75.20

^a) Assignments based on HSQC and HMBC spectra. ^b) Assignments may be interchanged.

Table 9. Selected $^1\text{H-NMR}$ Chemical Shifts [ppm] and Coupling Constants [Hz] of the Tetramers **8**, **14**, **18**, and **21** in (D_6)DMSO^a

Sequence	8	14	18	21		8	14	18	21
	UUAA	AAUU	UAUA	AUAU		UUAA	AAUU	UAUA	AUAU
H–C(5/I) or H–C(2/I)	8.15	5.63 ^b	8.16	5.64					
H–C(6/I) or H–C(8/I)	8.32	7.71	8.30	7.76	$J(5,6/I)$	–	8.1	–	8.1
HN(3/I) or H ₂ N–C(6/I)	7.34	11.41	7.35	11.46					
H–C(1'/I)	6.23	5.83	6.22	5.87					
H–C(2'/I)	5.40	4.99	5.37	5.00	$J(1',2'/I)$	2.8	2.4	2.7	2.5
H–C(3'/I)	5.20–5.16	4.94	5.143	4.96	$J(2',3'/I)$	6.1	6.4	6.2	6.5
H–C(4'/I)	4.31	4.09	4.26	4.15	$J(3',4'/I)$	2.2	3.4	2.7	2.7
H–C(5'/I)	4.84	4.75	4.80	4.802	$J(4',5'/I)$	6.2	6.4	6.3	6.6
HO–C(5'/I)	6.72	6.50	6.69	6.55	$J(5',\text{OH}/I)$	5.2	6.1	5.8	6.0
H–C(5/II) or H–C(2/II)	8.16	5.90 ^b	5.84	8.18					
HN(3/II) or H ₂ N–C(6/II)	7.62	11.70	11.66	7.64					
H–C(1'/II)	6.17	6.17	6.11	6.20					
H–C(2'/II)	5.47	5.26	5.23	5.48	$J(1',2'/II)$	2.6	1.6	1.0	2.5
H–C(3'/II)	5.20–5.16	4.98	4.94	5.19	$J(2',3'/II)$	6.4	6.6	6.6	6.6
H–C(4'/II)	4.22	4.04	4.03	4.22	$J(3',4'/II)$	2.7	3.2	3.1	3.0
H–C(5'/II)	4.81	4.70	4.69	4.815	$J(4',5'/II)$	7.1	9.0	9.1	6.7
HO–C(5'/II)	6.72	6.37	6.36	6.74	$J(4',\text{OH}/II)$	5.2	6.6	6.6	5.5
H–C(5/III) or H–C(2/III)	5.84	8.16	8.17	5.82					
HN(3/III) or H ₂ N–C(6/III)	11.61	7.63	7.65	11.70					
H–C(1'/III)	6.04	6.19	6.17	6.06					
H–C(2'/III)	5.20–5.16	5.45	5.43	5.205	$J(1',2'/III)$	1.0	3.1	3.0	1.2
H–C(3'/III)	4.90	5.22	5.165	4.92	$J(2',3'/III)$	6.6	6.3	6.2	6.7
H–C(4'/III)	3.98	4.27	4.23	4.00	$J(3',4'/III)$	3.3	2.7	2.7	3.5
H–C(5'/III)	4.64	4.94	4.86	4.70	$J(4',5'/III)$	9.0	6.4	6.9	9.0
HO–C(5'/III)	6.37	6.78	6.79	6.37	$J(4',\text{OH}/III)$	6.1	5.9	5.4	7.0
H–C(5/IV) or H–C(2/IV)	5.87	8.13	5.84	8.13					
HN(3/IV) or H ₂ N–C(6/IV)	11.61	7.52	11.66	7.53					
H–C(1'/IV)	6.06	6.11	6.01	6.13	$J(1',2'/IV)$	1.5	2.0	1.2	1.8
H–C(2'/IV)	5.20–5.16	5.60	5.160	5.61	$J(2',3'/IV)$	6.4	6.4	6.5	6.3
H–C(3'/IV)	4.72	5.05	4.70	5.07	$J(3',4'/IV)$	3.9	3.2	4.5	3.3
H–C(4'/IV)	4.01	4.11	3.98	4.13	$J(4',5'_a/IV)$	5.6	6.1	5.3	6.2
H _a –C(5'/IV)	3.793	3.76	3.77	3.78	$J(4',5'_b/IV)$	7.1	7.1	7.5	7.0
H _b –C(5'/IV)	3.765	3.68	3.75	3.69	$J(5'_a,5'_b/IV)$	10.5	10.5	10.5	10.5

^a) Assignments based on DQFCOSY, HSQC, and HMBC spectra. ^b) $^4J(5,\text{NH}/I) = ^4J(5,\text{NH}/II) = 2.0$ Hz.

additionally, 113.20, 112.56 (2s, 2 Me₂C); 26.92, 26.81, 25.14, 25.09 (4q, 2 Me₂C). HR-MALDI-MS: 637.1740 ($[M + \text{Na}]^+$, C₂₈H₃₀N₄NaO₁₂⁺; calc. 637.1758).

9-(6,7-Dideoxy-2,3-O-isopropylidene-β-D-allo-hept-6-ynofuranosyl)adenin-8-yl-(8 → 7'-C)-1-(6,7-dideoxy-2,3-O-isopropylidene-β-D-allo-hept-6-ynofuranosyl)uracil-6-yl-(6 → 7'-C)-1-(6,7-dideoxy-2,3-O-isopropylidene-β-D-allo-hept-6-ynofuranosyl)uracil (**12**). A soln. of **11** [2] (286 mg, 0.54 mmol), **10** (264 mg, 0.43 mmol), [Pd₂(dba)₃] (19.2 mg, 0.022 mmol), CuI (9.4 mg, 0.044 mmol), and P(fur)₃ (9.4 mg, 0.035 mmol) in degassed Et₃N/toluene 1:1 (15 ml) was stirred for 20 h at 25°. Evaporation and FC (CHCl₃/MeOH 20:1) gave the C-silylated trimer (282 mg; R_f (CHCl₃/MeOH 15:1) 0.22), which was dissolved in THF (10 ml), treated dropwise with a soln. of Bu₄NF · 3 H₂O (177 mg, 0.56 mmol) in THF (5 ml), and stirred for 2 h at 24°. Evaporation and FC (CHCl₃/MeOH 16:1) gave **12** (167 mg, 41%). Pale yellow solid. R_f (CHCl₃/MeOH 10:1) 0.26. M.p. 178° (dec.). $[\alpha]_{\text{D}}^{25} = +9.0$ (c = 1.0, CHCl₃). UV (CHCl₃):

Table 10. Selected ^{13}C -NMR Chemical Shifts [ppm] of the Tetramers **8**, **14**, **18**, and **21** in (D_6)DMSO^a

Sequence	8				14				18				21			
	UUAA	AAUU	UAUA	AUAU	UUAA	AAUU	UAUA	AUAU	UUAA	AAUU	UAUA	AUAU	UUAA	AAUU	UAUA	AUAU
C(2/I)	152.64	150.26	152.57	150.26	C(2/III)	149.50	153.61	153.55	149.85							
C(4/I)	148.05	163.11	148.50	163.09	C(4/III)	161.60	147.90	147.85	161.88							
C(5/I)	119.02	101.80	118.95	101.77	C(5/III)	108.10	118.94 ^b)	118.85	108.08							
C(6/I)	156.16 ^b)	142.44	156.08 ^b)	142.38	C(6/III)	135.65	156.05	155.99 ^b)	135.78							
C(8/I)	139.84	–	139.74	–	C(8/III)	–	132.17	132.15	–							
C(1'/I)	89.87	92.37	89.57	92.30	C(1'/III)	93.00	90.50	89.94	93.60							
C(2'/I)	83.20	83.43	83.08	83.41	C(2'/III)	83.20	82.27	82.33	83.13							
C(3'/I)	81.55	80.82	81.14	80.83	C(3'/III)	82.29	81.58	82.11	82.46							
C(4'/I)	87.83	87.96	87.55	87.96	C(4'/III)	89.87	87.72	87.43	89.90							
C(5'/I)	61.80	61.60	61.79	61.45	C(5'/III)	61.70	61.85	61.75	61.61							
C(6'/I)	95.26	101.85	101.45	95.41	C(6'/III)	102.51	95.16	101.22	96.36							
C(7'/I)	74.44	74.97	74.83 ^c)	73.37	C(7'/III)	73.40	73.36	74.93 ^c)	72.88							
C(2/II)	153.60	149.82	149.68	153.66	C(2/IV)	148.61	153.61	148.50	153.52							
C(4/II)	147.95	161.76	161.72	148.10	C(4/IV)	161.60	148.15	161.72	147.88							
C(5/II)	118.90	107.60	107.96	118.86 ^b)	C(5/IV)	107.80	118.77 ^b)	107.96	118.76 ^b)							
C(6/II)	156.09 ^b)	135.60	135.73	156.02	C(6/IV)	135.80	155.90	135.95	155.83							
C(8/II)	132.04	–	–	132.58	C(8/IV)	–	132.40	–	132.01							
C(1'/II)	90.00	93.40	94.00	89.90	C(1'/IV)	92.87	89.41	92.50	89.40							
C(2'/II)	82.29	83.43	83.33	82.31	C(2'/IV)	83.20	82.27	83.16	82.31							
C(3'/II)	81.55	82.36	81.68	81.48	C(3'/IV)	81.31	81.58	81.39	81.53							
C(4'/II)	87.72	90.15	89.94	87.72	C(4'/IV)	88.80	87.52	88.86	87.43							
C(5'/II)	61.78	61.69	61.60	61.75	C(5'/IV)	63.86	63.28	63.80	63.22							
C(6'/II)	101.43	96.79	96.66	101.56												
C(7'/II)	74.74	72.69	72.66	74.71												

^a) Assignments based on HSQC and HMBC spectra. ^b) ^c) Assignments may be interchanged.

287 (9000). IR (ATR): 3186w, 2987w, 2920w, 2260w, 1688s, 1601m, 1452m, 1375s, 1329m, 1301w, 1269m, 1212s, 1156m, 1067s, 1023s, 1002s, 852m, 820m, 760m, 709w, 663w. ^1H -NMR (500 MHz, (D_6)DMSO): see Table 7; additionally, 1.53, 1.48 (6 H), 1.31, 1.30 (6 H) (4s, 3 Me_2C). ^{13}C -NMR (125 MHz, (D_6)DMSO): see Table 8; additionally, 113.30 (s, 2 Me_2C); 113.16 (s, Me_2C); 27.04, 26.88, 26.81, 25.23, 25.11 (2 C) (5q, 3 Me_2C). HR-MALDI-MS: 966.2780 ($[M + \text{Na}]^+$, $\text{C}_{43}\text{H}_{45}\text{N}_9\text{NaO}_{16}$; calc. 966.2882).

2',3'-O-Isopropylidene-5'-O-(triisopropylsilyl)adenosin-8-yl-(8 \rightarrow 7'-C)-9-(6,7-dideoxy-2,3-O-isopropylidene- β -D-allo-hept-6-ynofuranosyl)adenin-8-yl-(8 \rightarrow 7'-C)-1-(6,7-dideoxy-2,3-O-isopropylidene- β -D-allo-hept-6-ynofuranosyl)uracil-6-yl-(6 \rightarrow 7'-C)-1-(6,7-dideoxy-2,3-O-isopropylidene- β -D-allo-hept-6-ynofuranosyl)uracil (**14**). A soln. of **13** [1] (121 mg, 0.21 mmol), **12** (130 mg, 0.138 mmol), $[\text{Pd}_2(\text{dba})_3]$ (12.9 mg, 0.014 mmol), CuI (5.3 mg, 0.028 mmol), and P(fur)₃ (5.3 mg, 0.022 mmol) in degassed Et₃N/toluene 1 : 1 (9 ml) was stirred for 24 h at 25°. Evaporation and FC ($\text{CHCl}_3/\text{MeOH}$ 20 : 1) gave **14** (110 mg, 57%). Pale yellow solid. R_f ($\text{CHCl}_3/\text{MeOH}$ 10 : 1) 0.28. M.p. 232° (dec.). $[\alpha]_{\text{D}}^{25} = +101.2$ ($c = 0.5$, CHCl_3). UV (CHCl_3): 292 (40000). IR (ATR): 3340w, 3191w, 2940w, 2865w, 2240w, 1688s, 1635s, 1599m, 1454w, 1374m, 1328m, 1299w, 1267m, 1213m, 1156m, 1067s, 854m, 798m, 763w, 710w, 682w. ^1H -NMR (500 MHz, (D_6)DMSO): see Table 9; additionally, 1.56, 1.48, 1.47, 1.46, 1.33, 1.30, 1.29, 1.28 (8s, 4 Me_2C); 0.91–0.89 (m, (Me_2CH)₃Si). ^{13}C -NMR (125 MHz, (D_6)DMSO): see Table 10; additionally, 113.49, 113.25, 113.10, 113.04 (4s, 4 Me_2C); 27.00, 26.84, 26.81, 26.76, 25.20, 25.10, 25.08, 25.05 (8q, 4 Me_2C); 17.58, 17.54 (2q, (Me_2CH)₃Si); 11.20 (d, (Me_2CH)₃Si). HR-MALDI-MS: 1427.527 ($[M + \text{Na}]^+$, $\text{C}_{65}\text{H}_{80}\text{N}_{14}\text{NaO}_{20}\text{Si}^+$; calc. 1427.534).

1-(6,7-Dideoxy-2,3-O-isopropylidene- β -D-allo-hept-6-ynofuranosyl)uracil-6-yl-(6 \rightarrow 7'-C)-9-(6,7-dideoxy-2,3-O-isopropylidene- β -D-allo-hept-6-ynofuranosyl)adenine (**16**). A soln. of **3** (440 mg, 0.8 mmol),

15 [2] (228 mg, 0.69 mmol), [Pd₂(dba)₃] (30.8 mg, 0.034 mmol), CuI (14.6 mg, 0.068 mmol), and P(fur)₃ (14.5 mg, 0.054 mmol) in degassed Et₃N/toluene 1:1 (12 ml) was stirred for 18 h at 24°. Evaporation and FC (CHCl₃/MeOH 30:1) gave the *C*-silylated dimer (305 mg; *R*_f (CHCl₃/MeOH 15:1) 0.25), which was dissolved in THF (9 ml), treated dropwise with a soln. of Bu₄NF·3 H₂O (205 mg, 0.64 mmol) in THF (6 ml), and stirred for 4 h at 24°. Evaporation and FC (CHCl₃/MeOH 20:1) gave **16** (165 mg, 37%). Pale yellow solid. *R*_f (CHCl₃/MeOH 15:1) 0.20. M.p. 200° (dec.). [α]_D²⁵ = –89.0 (*c* = 0.5, CHCl₃). UV (CHCl₃): 265 (24300). IR (ATR): 3441w, 3324w, 3263w, 3206w, 2987w, 2864w, 2240w, 1685s, 1646s, 1596m, 1470w, 1376s, 1333w, 1259m, 1197m, 1155m, 1124w, 1085s, 1060s, 970w, 865m, 796w, 761m, 692w, 651m. ¹H-NMR (300 MHz, (D₆)DMSO): see Table 5; additionally, 1.54, 1.40, 1.34, 1.24 (4s, 2 Me₂C). ¹³C-NMR (75 MHz, (D₆)DMSO): see Table 6; additionally, 113.21, 112.44 (2s, 2 Me₂C); 27.00, 26.80, 25.25, 25.15 (4q, 2 Me₂C). HR-MALDI-MS: 660.2014 ([*M* + Na]⁺, C₂₉H₃₁N₇NaO₁₀⁺; calc. 660.2030).

9-(6,7-Dideoxy-2,3-O-isopropylidene-β-D-*allo*-hept-6-ynofuranosyl)adenin-8-yl-(8 → 7'-C)-1-(6,7-dideoxy-2,3-O-isopropylidene-β-D-*allo*-hept-6-ynofuranosyl)uracil-6-yl-(6 → 7'-C)-9-(6,7-dideoxy-2,3-O-isopropylidene-β-D-*allo*-hept-6-ynofuranosyl)adenine (**17**). A soln. of **11** (95 mg, 0.18 mmol), **16** (95 mg, 0.15 mmol), [Pd₂(dba)₃] (13.7 mg, 0.015 mmol), CuI (5.7 mg, 0.03 mmol), and P(fur)₃ (5.7 mg, 0.024 mmol) in degassed Et₃N/toluene 1:1 (4 ml) was stirred for 18 h at 23°. Evaporation and FC (CHCl₃/MeOH 15:1) gave the *C*-silylated trimer (305 mg; *R*_f (CHCl₃/MeOH 15:1) 0.22), which was dissolved in THF (10 ml), treated dropwise with a soln. of Bu₄NF·3 H₂O (57 mg, 0.18 mmol) in THF (2 ml) and stirred for 1 h at 23°. Evaporation and FC (CHCl₃/MeOH 15:1) gave **17** (80 mg, 55%). *R*_f (CHCl₃/MeOH 10:1) 0.21. M.p. 239° (dec.). [α]_D²⁵ = –46.9 (*c* = 0.5, CHCl₃). UV (CHCl₃): 268 (26300). IR (ATR): 3320w, 3188w, 2987w, 2940w, 2240w, 1695m, 1639s, 1598s, 1432w, 1375m, 1330m, 1300w, 1269w, 1213m, 1156m, 1077s, 1004m, 852m, 797w, 761w, 707w, 646w. ¹H-NMR (500 MHz, (D₆)DMSO): see Table 7; additionally, 1.54, 1.52, 1.44, 1.33, 1.30, 1.28 (6s, 3 Me₂C). ¹³C-NMR (125 MHz, (D₆)DMSO): see Table 8; additionally, 113.26, 113.22, 112.66 (3s, 3 Me₂C); 26.93, 26.87, 26.66, 25.13, 25.11, 25.05 (6q, 3 Me₂C). HR-MALDI-MS: 989.3233 ([*M* + Na]⁺, C₄₄H₄₆N₁₂NaO₁₄⁺; calc. 989.3154).

2',3'-O-Isopropylidene-5'-O-(triisopropylsilyl)uridin-6-yl-(6 → 7'-C)-9-(6,7-dideoxy-2,3-O-isopropylidene-β-D-*allo*-hept-6-ynofuranosyl)adenin-8-yl-(8 → 7'-C)-1-(6,7-dideoxy-2,3-O-isopropylidene-β-D-*allo*-hept-6-ynofuranosyl)uracil-6-yl-(6 → 7'-C)-9-(6,7-dideoxy-2,3-O-isopropylidene-β-D-*allo*-hept-6-ynofuranosyl)adenine (**18**). A soln. of **7** (37 mg, 0.065 mmol), **17** (42 mg, 0.043 mmol), [Pd₂(dba)₃] (3.9 mg, 0.0043 mmol), CuI (1.6 mg, 0.0086 mmol), and P(fur)₃ (1.6 mg, 0.007 mmol) in degassed Et₃N/toluene 1:1 (6 ml) was stirred for 16 h at 25°. Evaporation and FC (CHCl₃/MeOH 10:1) gave **18** (30 mg, 50%). Pale yellow solid. *R*_f (CHCl₃/MeOH 10:1) 0.22. M.p. 225° (dec.). [α]_D²⁵ = –27.3 (*c* = 0.5, CHCl₃). UV (CHCl₃): 276 (17600). IR (ATR): 3340w, 3188w, 2927w, 2864w, 2240w, 1694m, 1639m, 1596m, 1444w, 1374m, 1330w, 1302w, 1264w, 1214m, 1156w, 1067s, 867m, 796m, 761w, 683w, 647w. ¹H-NMR (500 MHz, (D₆)DMSO): see Table 9; additionally, 1.53 (6 H), 1.44, 1.38, 1.33, 1.31, 1.28, 1.23 (7s, 4 Me₂C); 1.02–0.97 (*m*, (Me₂CH)₃Si). ¹³C-NMR (125 MHz, (D₆)DMSO): see Table 10; additionally, 113.49, 113.25, 113.10, 113.04 (4s, 4 Me₂C); 27.00, 26.84, 26.81, 26.76, 25.20, 25.10, 25.08, 25.05 (8q, 4 Me₂C); 17.58, 17.54 (2q, (Me₂CH)₃Si); 11.20 (*d*, (Me₂CH)₃Si). HR-MALDI-MS: 1427.537 ([*M* + Na]⁺, C₆₅H₈₀N₁₄NaO₂₀Si⁺; calc. 1427.534).

9-(6,7-Dideoxy-2,3-O-isopropylidene-β-D-*allo*-hept-6-ynofuranosyl)adenin-8-yl-(8 → 7'-C)-1-(6,7-dideoxy-2,3-O-isopropylidene-β-D-*allo*-hept-6-ynofuranosyl)uracil (**19**). A soln. of **11** (529 mg, 1.0 mmol), **9** (256 mg, 0.83 mmol), [Pd₂(dba)₃] (37 mg, 0.042 mmol), CuI (18.4 mg, 0.084 mmol), and P(fur)₃ (17.9 mg, 0.067 mmol) in degassed Et₃N/toluene 1:1 (15 ml) was stirred for 20 h at 25°. Evaporation and FC (CHCl₃/MeOH 20:1) gave the *C*-silylated dimer (305 mg; *R*_f (CHCl₃/MeOH 15:1) 0.30), which was dissolved in THF (20 ml), treated dropwise with a soln. of Bu₄NF·3 H₂O (286 mg, 0.88 mmol) in THF (7 ml) and stirred for 30 min at 23°. Evaporation and FC (CHCl₃/MeOH 20:1) gave **19** (384 mg, 72%). Pale yellow solid. *R*_f (CHCl₃/MeOH 10:1) 0.33. M.p. 196° (dec.). [α]_D²⁵ = –35.9 (*c* = 1.0, CHCl₃). UV (CHCl₃): 296 (5600). IR (ATR): 3360w, 3178m, 2986w, 2864w, 2240w, 1689s, 1659s, 1574w, 1448w, 1375m, 1329m, 1303m, 1269m, 1214m, 1155m, 1073s, 1023s, 1004s, 969m, 853m, 822m, 756m, 700w, 663w. ¹H-NMR (300 MHz, (D₆)DMSO): see Table 5; additionally, 1.53, 1.50, 1.31 (6 H) (3s, 2 Me₂C). ¹³C-NMR (75 MHz, (D₆)DMSO): see Table 6; additionally, 113.36, 113.20 (2s, 2 Me₂C); 27.05, 26.92, 25.14 (2 C) (3q, 2 Me₂C). HR-MALDI-MS: 660.2008 ([*M* + Na]⁺, C₂₉H₃₁N₇NaO₁₀⁺; calc. 660.2030).

1-(6,7-Dideoxy-2,3-O-isopropylidene- β -D-allo-hept-6-ynofuranosyl)uracil-6-yl-(6 \rightarrow 7'-C)-9-(6,7-dideoxy-2,3-O-isopropylidene- β -D-allo-hept-6-ynofuranosyl)adenin-8-yl-(8 \rightarrow 7'-C)-1-(6,7-dideoxy-2,3-O-isopropylidene- β -D-allo-hept-6-ynofuranosyl)uracil (**20**). A soln. of **3** (158 mg, 0.29 mmol), **19** (147 mg, 0.23 mmol), [Pd₂(dba)₃] (12.5 mg, 0.014 mmol), CuI (6.0 mg, 0.028 mmol), and P(fur)₃ (6.4 mg, 0.022 mmol) in degassed Et₃N/toluene 1:1 (10 ml) was stirred for 16 h at 25°. Evaporation and FC (CHCl₃/MeOH 16:1) gave the C-silylated trimer (305 mg; R_f (CHCl₃/MeOH 15:1) 0.25), which was dissolved in THF (10 ml), treated dropwise with a soln. of Bu₄NF · 3 H₂O (72 mg, 0.22 mmol) in THF (5 ml) and stirred for 3 h at 23°. Evaporation and FC (CHCl₃/MeOH 10:1) gave **20** (128 mg, 70%). Pale yellow solid. R_f (CHCl₃/MeOH 10:1) 0.27. M.p. 240° (dec.). [α]_D²⁵ = -17.2 (c = 1.0, CHCl₃). UV (CHCl₃): 294 (9100). IR (ATR): 3320w, 3188w, 2954w, 2864w, 2240w, 1687s, 1599m, 1452m, 1375s, 1328w, 1301w, 1269m, 1214s, 1155w, 1074s, 854m, 727m, 665w. ¹H-NMR (500 MHz, (D₆)DMSO): see Table 7; additionally, 1.55, 1.50, 1.36, 1.33, 1.32, 1.23 (6s, 3 Me₂C). ¹³C-NMR (125 MHz, (D₆)DMSO): see Table 8; additionally, 113.48, 113.18, 112.47 (3s, 3 Me₂C); 26.99, 26.93, 26.69, 25.18, 25.14, 25.13 (6q, 3 Me₂C). HR-MALDI-MS: 966.277 ([M + Na]⁺, C₄₃H₄₅N₉NaO₁₆; calc. 966.288).

2',3'-O-Isopropylidene-5'-O-(triisopropylsilyl)adenosin-8-yl-(8 \rightarrow 7'-C)-1-(6,7-dideoxy-2,3-O-isopropylidene- β -D-allo-hept-6-ynofuranosyl)uracil-6-yl-(6 \rightarrow 7'-C)-9-(6,7-dideoxy-2,3-O-isopropylidene- β -D-allo-hept-6-ynofuranosyl)adenin-8-yl-(8 \rightarrow 7'-C)-1-(6,7-dideoxy-2,3-O-isopropylidene- β -D-allo-hept-6-ynofuranosyl)uracil (**21**). A soln. of **13** (86 mg, 0.15 mmol), **20** (91 mg, 0.096 mmol), [Pd₂(dba)₃] (9.2 mg, 0.01 mmol), CuI (3.8 mg, 0.02 mmol), and P(fur)₃ (3.8 mg, 0.016 mmol) in degassed Et₃N/toluene 1:1 (6 ml) was stirred for 20 h at 25°. Evaporation and FC (CHCl₃/MeOH 20:1) gave **21** (82 mg, 61%). Pale yellow solid. R_f (CHCl₃/MeOH 10:1) 0.31. M.p. 219° (dec.). [α]_D²⁵ = -5.1 (c = 1.0, CHCl₃). UV (CHCl₃): 294 (9200). IR (ATR): 3332w, 3200w, 2941w, 2865w, 2240w, 1690s, 1634s, 1597m, 1453w, 1374m, 1328m, 1297w, 1268m, 1214m, 1156m, 1068s, 865m, 798w, 759m, 711w, 682w. ¹H-NMR (500 MHz, (D₆)DMSO): see Table 9; additionally, 1.53, 1.49 (6 H), 1.38, 1.31, 1.30, 1.29, 1.25 (7s, 4 Me₂C); 0.91–0.89 (m, (Me₂CH)₃Si). ¹³C-NMR (125 MHz, (D₆)DMSO): see Table 10; additionally, 113.36, 113.06, 112.99, 112.56 (4s, 4 Me₂C); 26.89, 26.79 (2 C), 26.56, 25.07 (2 C), 25.04 (2 C) (5q, 4 Me₂C); 17.55, 17.50 (2q, (Me₂CH)₃Si); 11.15 (d, (Me₂CH)₃Si). HR-MALDI-MS: 1427.528 ([M + Na]⁺, C₆₅H₈₀N₁₄NaO₂₀Si⁺; calc. 1427.534).

REFERENCES

- [1] X. Zhang, B. Bernet, A. Vasella, *Helv. Chim. Acta* **2006**, *89*, 2861.
- [2] P. K. Bhardwaj, A. Vasella, *Helv. Chim. Acta* **2002**, *85*, 699.
- [3] H. Gunji, A. Vasella, *Helv. Chim. Acta* **2000**, *83*, 1331.
- [4] S. Eppacher, N. Solladié, A. Vasella, *Helv. Chim. Acta* **2004**, *87*, 2926.
- [5] S. Eppacher, N. Solladié, B. Bernet, A. Vasella, *Helv. Chim. Acta* **2000**, *83*, 1311.
- [6] B. Bernet, A. Vasella, *Helv. Chim. Acta* **2000**, *83*, 995; B. Bernet, A. Vasella, *Helv. Chim. Acta* **2000**, *83*, 2055.
- [7] H. Gunji, A. Vasella, *Helv. Chim. Acta* **2000**, *83*, 2975.
- [8] G. Rossé, U. Séquin, H. Mett, P. Furet, P. Traxler, H. Fretz, *Helv. Chim. Acta* **1997**, *80*, 653.
- [9] T. Pehk, A. Uri, *Bioorg. Med. Chem. Lett.* **1997**, *7*, 2159.
- [10] D. J. Maly, J. A. Allen, K. M. Shokat, *J. Am. Chem. Soc.* **2004**, *126*, 9160.
- [11] J. S. Chen, R. B. Shirts, *J. Phys. Chem.* **1985**, *89*, 1643.
- [12] B. Peterson, Ph. D. Thesis, University of California at Los Angeles, 1994.
- [13] S. Eppacher, P. K. Bhardwaj, B. Bernet, J. L. B. Gala, T. Knöpfel, A. Vasella, *Helv. Chim. Acta* **2004**, *87*, 2969.
- [14] A. Dunger, H.-H. Limbach, K. Weisz, *J. Am. Chem. Soc.* **2000**, *122*, 10109.
- [15] F. Mohamadi, N. G. J. Richards, W. C. Guida, R. Liskamp, C. Caufield, M. Lipton, G. Chang, T. Hendrickson, W. C. Still, *J. Comput. Chem.* **1990**, *11*, 440.

Received November 29, 2006